Progress in Neurobiology xxx (xxxx) xxx

Contents lists available at ScienceDirect

Progress in Neurobiology

journal homepage: www.elsevier.com/locate/pneurobio

Original Research Article

Human hippocampal connectivity is stronger in olfaction than other sensory systems

Guangyu Zhou [a,*], Jonas K. Olofsson [b,c,d], Mohamad Z. Koubeissi [f], Georgios Menelaou [b], Joshua Rosenow [e], Stephan U. Schuele [a], Pengfei Xu [g,h,i], Joel L. Voss [a,j,k], Gregory Lane [a], Christina Zelano [a,*]

[a] Department of Neurology, Northwestern University Feinberg School of Medicine, Chicago, IL, USA
[b] Department of Psychology, Stockholm University, Stockholm, Sweden
[c] Emotional Brain Institute, Nathan S. Kline Institute, Orangeburg, NY, USA
[d] Department of Child and Adolescent Psychiatry, New York University School of Medicine, New York, NY, USA
[e] Department of Neurosurgery, Northwestern University Feinberg School of Medicine, Chicago, IL, USA
[f] Department of Neurology, George Washington University, Washington DC, USA
[g] Beijing Key Laboratory of Applied Experimental Psychology, Faculty of Psychology, Beijing Normal University, Beijing, China
[h] Center for Neuroimaging, Shenzhen Institute of Neuroscience, Shenzhen, China
[i] Guangdong-Hong Kong-Macao Greater Bay Area Research Institute for Neuroscience and Neurotechnologies, Kwun Tong, Hong Kong, China
[j] Department of Medical Social Sciences, Northwestern University Feinberg School of Medicine, Chicago, IL, USA
[k] Department of Psychiatry and Behavioral Sciences, Northwestern University Feinberg School of Medicine, Chicago, IL, USA

ARTICLE INFO

Keywords:
Hippocampal network
Olfactory system
Functional connectivity
fMRI
iEEG

ABSTRACT

During mammalian evolution, primate neocortex expanded, shifting hippocampal functional networks away from primary sensory cortices, towards association cortices. Reflecting this rerouting, human resting hippocampal functional networks preferentially include higher association cortices, while those in rodents retained primary sensory cortices. Research on human visual, auditory and somatosensory systems shows evidence of this rerouting. Olfaction, however, is unique among sensory systems in its relative structural conservation throughout mammalian evolution, and it is unknown whether human primary olfactory cortex was subject to the same rerouting. We combined functional neuroimaging and intracranial electrophysiology to directly compare hippocampal functional networks across human sensory systems. We show that human primary olfactory cortex—including the anterior olfactory nucleus, olfactory tubercle and piriform cortex—has stronger functional connectivity with hippocampal networks at rest, compared to other sensory systems. This suggests that unlike other sensory systems, olfactory-hippocampal connectivity may have been retained in mammalian evolution. We further show that olfactory-hippocampal connectivity oscillates with nasal breathing. Our findings suggest olfaction might provide insight into how memory and cognition depend on hippocampal interactions.

1. Introduction

Learning and memory of perceptual events are indispensable features of the mammalian brain, enabled by connectivity between the hippocampus and the cortex. The overall organization of hippocampal-cortical networks is thought to be well-preserved across mammalian species (Allen and Fortin, 2013; Gass et al., 2014; Liska et al., 2015; Lu et al., 2012; Mechling et al., 2014; Schwarz et al., 2013). However, during mammalian evolution, primates (including humans) experienced a profound expansion of neocortex that reorganized these networks, fundamentally separating humans from other mammals (Buckner and Krienen, 2013). Specifically, human hippocampal networks were rerouted away from primary sensory cortices, towards association cortices. Reflecting this change, recent functional neuroimaging studies that directly compared rodent and human resting functional hippocampal networks found that while rodent hippocampal networks include primary sensory cortices, those in humans instead preferentially include association cortices (Bergmann et al., 2016; Kahn et al., 2008; Libby et al., 2012). Though such effects were shown in the visual, auditory and somatosensory systems, a fundamental question is whether

* Corresponding authors.
E-mail addresses: guangyu.zhou@northwestern.edu (G. Zhou), c-zelano@northwestern.edu (C. Zelano).

https://doi.org/10.1016/j.pneurobio.2021.102027
Received 4 November 2020; Received in revised form 20 January 2021; Accepted 21 February 2021
Available online 25 February 2021

there are exceptions to this general principle of human sensory-hippocampal network reorganization. If any human sensory system retained direct connectivity with the hippocampus, this might have important implications for our understanding of human memory, which depends on hippocampal interactions. Olfaction provides a critical point of comparison, as it is typically not considered in theoretical frameworks of cognitive evolution or overall cortical organization (Buckner and Krienen, 2013; Margulies et al., 2016; Mesulam, 1998), but is instead often regarded as preserved in mammalian evolution (Herrick, 1933; McGann, 2017; Striedter and Northcutt, 2020). If the human hippocampus preserved connectivity with any primary sensory area, we reasoned it would likely be found in olfaction.

Connectivity between the hippocampus and cortical areas differs between rodents and primates, both anatomically and functionally. Anatomically, in both rodents and primates, parahippocampal regions, which provide access to the hippocampus, are projection sites for higher sensory and association areas (Aronoff et al., 2010; Burwell, 2006; Burwell and Amaral, 1998; Wang et al., 2012), but only in the rodent does the parahippocampus exhibit direct anatomical connections with primary visual, auditory and somatosensory cortices (Kahn et al., 2008; Libby et al., 2012; Ranganath and Ritchey, 2012). Functionally, in both rodents and humans, parahippocampal regions exhibit resting functional connectivity with higher association areas (Gass et al., 2014; Kahn et al., 2008; Libby et al., 2012; Liska et al., 2015; Logothetis et al., 2012; Madore et al., 2016; Mechling et al., 2014; Ranganath and Ritchey, 2012; Schwarz et al., 2013; Tambini et al., 2017), but only rodent parahippocampus exhibits functional connectivity with primary visual, auditory and somatosensory cortices (Bergmann et al., 2016). These findings suggest that in humans, primary sensory information was rerouted via expanded and new association cortices before arriving at the hippocampus. Cortical evolution thus extended the "synaptic leash" from sensation to cognition, which likely allowed for a greater cognitive and behavioral flexibility (Mesulam, 1998). These studies, however, focused on the visual, auditory and somatosensory systems, and did not consider the olfactory system.

The question of whether the human olfactory system participated in the reorganization described above remains unanswered. Direct human anatomical and functional evidence is scant in the field of olfaction. Anatomically, connectivity between primary olfactory areas and the hippocampal formation has been well established in rodents, but whether this is true in humans is unknown. In rodents, both the olfactory bulb and piriform cortex project to the entire extent of the entorhinal cortex (Barkai and Saar, 2001; Haberly, 2001), which in turn projects to the hippocampus. As primary olfactory cortex includes a collection of brain areas that receive direct input from the olfactory bulb (Carmichael et al., 1994; Ennis et al., 2015; Gottfried, 2010; Illig and Wilson, 2009; Lane et al., 2020; Mainland et al., 2014; Porada et al., 2019; Price, 2009, 1990; Vaughan and Jackson, 2014; Wilson and Sullivan, 2003), rodent entorhinal cortex is a substantial part of primary olfactory cortex. The organization of primary olfactory cortex may differ somewhat in primates and humans (Lane et al., 2020). In macaques, the olfactory bulb projects to a comparatively very small rostral part of the entorhinal cortex, and it is unknown whether piriform cortex also projects here (Carmichael et al., 1994). In humans, though we lack direct anatomical evidence for bulbar or piriform projections to the entorhinal cortex, a handful of magnetic resonance structural and diffusion-tensor-based studies indirectly suggest that some may exist (Gonçalves Pereira et al., 2005; Héctor et al., 2019; Milardi et al., 2017). Thus, in humans, we cannot rely on current anatomical evidence to determine whether connectivity between the hippocampus and olfactory areas was rerouted as in other sensory systems. Resting-state functional magnetic resonance imaging (rsfMRI) techniques have contributed to our understanding of intrinsic functional networks in the human brain (Cabral et al., 2014; Fox et al., 2005; Greicius et al., 2003; van den Heuvel and Hulshoff Pol, 2010), and have been used to provide support for the notion that hippocampal functional networks were rerouted in visual, auditory and somatosensory systems during mammalian evolution (Bergmann et al., 2016). In olfaction, numerous previous studies have explored intrinsic functional networks of the human olfactory system (Arnold et al., 2020; Banks et al., 2016; Cecchetto et al., 2019; Fjaeldstad et al., 2017; Karunanayaka et al., 2017, 2014; Kiparizoska and Ikuta, 2017; Kollndorfer et al., 2015; Krusemark and Li, 2012; Nigri et al., 2013; Peter et al., 2021; Sreenivasan et al., 2017; Sunwoo et al., 2015). Of these, the few that separately considered piriform cortex found functional connectivity with hippocampus (Karunanayaka et al., 2017; Lu et al., 2019; Tobia et al., 2016; Zhou et al., 2019a). A number of studies have reported unique qualities of olfactory memories compared to visual/auditory memories (Arshamian et al., 2013; Chu and Downes, 2000; Cornell Kärnekull et al., 2020; Miles and Berntsen, 2011; Saive et al., 2014; Willander and Larsson, 2006), and it has been argued that "the strong anatomical connection between olfactory and memory structures makes olfaction a privileged sense for accessing memories"(Saive et al., 2014). However, despite the prevalent hypothesis that the olfactory cortex has a stronger functional integration with the hippocampus compared to other sensory cortices, the strength of olfactory-hippocampal networks relative to other sensory systems has not been directly compared. It is therefore unknown whether resting human olfactory-hippocampal networks underwent evolutionary rerouting similar to what is proposed for other sensory modalities.

How can human olfactory-hippocampal networks be characterized? One possibility is that, similar to other sensory systems, resting olfactory-hippocampal networks were rerouted from primary sensory cortex to preferentially include higher association cortices. Another possibility is that, unlike other human sensory systems, olfactory-hippocampal networks maintained the involvement of primary sensory cortex, as in rodents. Given anatomical and evolutionary characteristics of the olfactory system, and the high level of conservation of the overall organizational properties of human and rodent olfactory systems, we hypothesized that the evolutionary rerouting of human neocortical hippocampal networks to higher association cortices did not include the olfactory system. If true, this would suggest that human olfactory-hippocampal networks include primary olfactory cortical areas, unlike other sensory systems. Furthermore, such a result would support the notion that primate cortical expansion was driven not by evolutionary pressures related to olfactory processing, but by processing demands in other senses (e.g., visual, auditory and somatosensory).

Unlike other sensory systems, olfactory perception is inextricably tied to respiration. Information about olfactory stimuli is processed rhythmically in the olfactory bulb and piriform cortex, and responses in these areas are tied to sniff phase (Carey and Wachowiak, 2011; Kepecs et al., 2006; Rebello et al., 2014; Shusterman et al., 2011; Smear et al., 2011). Furthermore, activity in olfactory cortical areas, in hippocampus and in some neocortical areas, has been found to oscillate with respiratory rhythms even at rest (Heck et al., 2016; Liu et al., 2017; Lockmann and Tort, 2018; Lockmann et al., 2016; Nguyen Chi et al., 2016; Tort et al., 2018; Yanovsky et al., 2014; Zelano et al., 2016). This suggests that respiratory rhythmicity might impact not only local activity, but also network coherence, perhaps including olfactory-hippocampal networks (Macrides, 1975; Macrides et al., 1982; Vanderwolf, 2001, 1992). In humans, however, respiratory rhythmicity of resting olfactory-hippocampal networks remains unexplored. We hypothesized that, if human olfactory-hippocampal networks include primary olfactory cortex, then connectivity between piriform cortex and hippocampus should be modulated by respiration, even at rest.

Here, we used rsfMRI and intracranial electroencephalography (iEEG) to test two hypotheses about resting human olfactory-hippocampal networks. The use of two complimentary techniques which show striking similarities in their estimates of intrinsic functional networks (Fox et al., 2018; Kucyi et al., 2018) allowed us both to examine connectivity across all primary olfactory subregions, and to assess connectivity using a direct measure of neural activity. First, we used whole-brain rsfMRI to test the hypothesis that human

olfactory-hippocampal functional networks include primary sensory cortex, unlike other sensory systems. We directly compared the strength of connectivity between the hippocampus and olfactory sensory cortex to that between the hippocampus and somatosensory, visual and auditory sensory cortices. This analysis was repeated using resting state iEEG techniques, which provided coverage of the hippocampus and primary olfactory and auditory cortices, and allowed us to validate rsfMRI findings using a direct measure of neural activity. Second, we used iEEG to test the hypothesis that resting connectivity between olfactory cortex and hippocampus is modulated by respiratory rhythms, which would suggest a functional link between resting connectivity and passive sensory sampling behaviors, even at rest.

2. Results

To directly compare human sensory cortical–hippocampal functional connectivity across the olfactory, somatosensory, visual and auditory systems, we acquired whole-brain rsfMRI signals from 25 healthy participants. Whole-brain acquisition allowed direct comparison of simultaneous hippocampal connectivity across sensory systems. To examine human olfactory-hippocampal connectivity at the neural level, we used iEEG techniques to record local field potential signals during rest, directly from piriform cortex, auditory cortex and hippocampus, from 8 participants undergoing an invasive evaluation for epilepsy. These targeted recordings allowed quantification and comparison of olfactory and auditory hippocampal connectivity with high temporal precision, and validation of our fMRI findings. iEEG methods also allowed us to examine the temporal dynamics of phase synchrony between piriform and hippocampus over the respiratory cycle.

2.1. Primary olfactory cortex maintains stronger hippocampal connectivity than do other primary sensory cortices

We first tested the hypothesis that resting functional connectivity between piriform cortex and the hippocampus would be stronger than that between other primary sensory cortices and the hippocampus. We compared hippocampal connectivity across sensory cortices, including primary visual (V1 and V2), auditory (A1 and A2), somatosensory (S1) (Luna et al., 2005) and olfactory (piriform) cortices. Resting fMRI-based functional connectivity (Greicius et al., 2003) was computed between the hippocampus (seed region of interest (ROI)) and each primary sensory cortical target ROI (Fig. 1A). ROIs were obtained from *FSL*'s standard Harvard-Oxford atlas (S1, A1 and A2) (Jenkinson et al., 2012) and *Freesurfer*'s labels (V1 and V2) (Desikan et al., 2006) (See **Materials and Methods** for details). The piriform cortex ROI was manually drawn on a Montreal Neurological Institute (MNI) brain according to a human brain atlas that provides a particularly detailed consideration of medial limbic structures (Mai et al., 2015; Zhou et al., 2019a). To calculate the functional connectivity between each pair of ROIs, we extracted the fMRI time series of all voxels within each ROI and averaged them, which resulted in a single time series for each ROI for each participant. We then calculated the Pearson correlation coefficient between all pairs of time series for each participant. Finally, the correlation coefficients were converted to z scores using Fisher z-transformation. To look for differences in connectivity between the hippocampal seed ROIs (left and right hippocampus) and each primary sensory cortex, we first performed a two-way repeated-measures analysis of variance (ANOVA) with hemisphere (left and right) and region (visual, somatosensory, auditory and olfactory cortices) as factors (Fig. 1A). Multiple comparisons of the

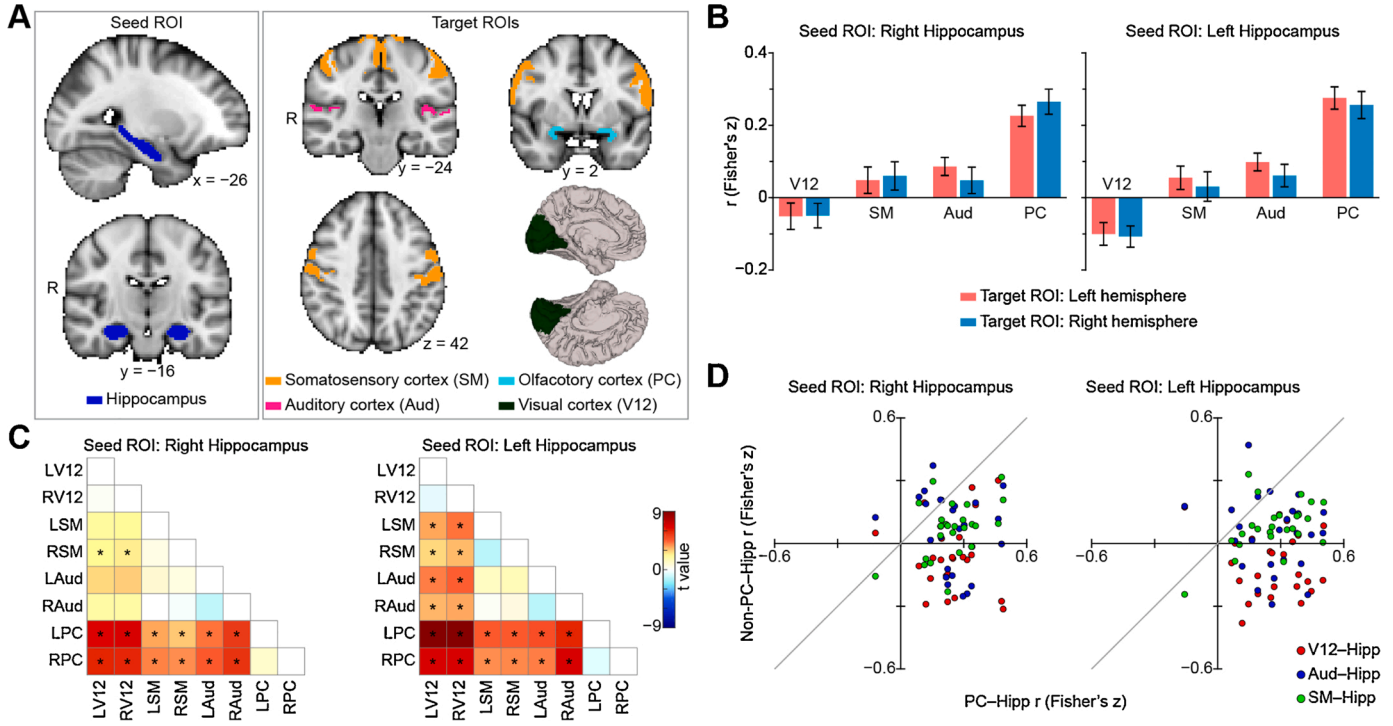

Fig. 1. Resting fMRI functional connectivity between hippocampus and sensory cortices. (A). Regions of interest on a Montreal Neurological Institute standard brain. The seed regions include left and right hippocampus, and the target regions include left and right visual, somatosensory, auditory and olfactory cortices. (B). Hippocampal connectivity across sensory systems. Bar plots indicate the average correlation between seed and target region across participants (N = 25), and error bars indicate standard error. (C). T value maps of two-tailed paired *t*-tests (N = 25). Asterisks indicate statistical significance ($P < 0.05$, FDR corrected). (D). Hippocampal connectivity at the individual level. A scatter plot of the olfactory-hippocampal functional connectivity (PC–Hipp) plotted against the non-olfactory-hippocampal functional connectivity (Non-PC–Hipp). Each dot represents a data point from one participant. The left and right hemispheres of each target region were averaged. Each participant has three data points (red (visual cortex); blue (auditory cortex); and green (somatosensory cortex)). Dots below the light gray diagonal line indicate olfactory-hippocampal connectivity is greater than non-olfactory-hippocampal connectivity. R, right hemisphere; Hipp, hippocampus; V12, V1 and V2; Aud, Heschl's gyrus and planum temporale; PC, piriform cortex; SM, precentral and postcentral gyrus.

ANOVA analysis across seed ROIs (left and right hippocampus) were corrected using the Bonferroni method. We found that hippocampal connectivity differed across primary sensory cortices, with similar effects across hemispheres as revealed by a main effect of region for both left ($F_{3,72}$ = 25.80, P = 1.92e−11) and right ($F_{3,72}$ = 16.37, P = 3.29e−8) hippocampus seed ROIs (Fig. 1B). The analysis revealed no statistically significant main effect of hemisphere on hippocampal connectivity (left hippocampus seed ROI: $F_{1,24}$ = 2.66, P = 0.12; right hippocampus seed ROI: $F_{1,24}$ = 0.073, P = 0.79). We found no interaction between hemisphere and region (left hippocampus seed ROI: $F_{3,72}$ = 0.31, P = 0.82; right hippocampus seed ROI: $F_{3,72}$ = 1.29, P = 0.29). Post-hoc two-tailed paired t-test analyses (N = 25) conducted between all target ROIs (Fig. 1C) showed that connectivity between the hippocampus and olfactory cortex was stronger than hippocampal connectivity with visual, auditory or somatosensory cortices (P < 0.05, false discovery rate (FDR) corrected; Fig. 1C). These effects were highly consistent across participants (Fig. 1D) and support our hypothesis that human olfactory-hippocampal functional networks include primary sensory cortex, unlike other sensory systems.

Though our original analysis focused on piriform cortex, the largest and most studied subregion of primary olfactory cortex (Allison, 1954; Carmichael et al., 1994; Feher, 2017; Gottfried, 2010; Mai and Paxinos, 2012; Price, 2009; Uyematsu, 1921; Vaughan and Jackson, 2014), the olfactory bulb also projects monosynaptically to several other cortical areas, which are also considered part of primary olfactory cortex, including the anterior olfactory nucleus and the olfactory tubercle. To determine if olfactory-hippocampal networks include other primary olfactory cortical regions, we next computed functional connectivity between these regions and the hippocampus. ROIs of the anterior olfactory nucleus and the olfactory tubercle were drawn on the MNI brain according to the human brain atlas (Mai et al., 2015). Since we didn't find any main effect of hemisphere in the previous analyses, we averaged the time series of the left and right hemispheres for each ROI before calculating the correlation coefficient across ROIs. We found stronger connectivity between the hippocampus and each primary olfactory region, compared to each non-olfactory primary sensory cortex (one-way repeated-measures ANOVA; $F_{6,144}$ = 18.50, P = 7.77e−16; Fig. 2A top), suggesting these effects were not specific to piriform cortex (two-tailed paired t-test; P < 0.05, FDR corrected; Fig. 2A bottom), and included other primary olfactory regions.

Having established unique resting functional connectivity between primary olfactory cortex and the hippocampus, we next asked whether resting olfactory connectivity is preferential to any particular subregion of the hippocampus. In other sensory systems, hippocampal networks are thought to involve two distinct, parallel pathways of cortical inputs (Ho and Burwell, 2014; Ranganath and Ritchey, 2012). An anterior pathway brings object-related information to the hippocampus via the perirhinal cortex, while a posterior pathway brings context-related information to the hippocampus through the parahippocampal and retrosplenial cortices (Buckley and Gaffan, 1997; Choi et al., 2020; Colombo et al., 1998; Epstein, 2008; Fanselow and Dong, 2010; Henderson et al., 2008; Howell et al., 2020; Janzen and Van Turennout, 2004; Moser and Moser, 1998; Murray and Richmond, 2001; Norman and Eacott, 2005; Strange et al., 2014; Taylor et al., 2006). It is unclear how human olfactory networks are aligned with these pathways. In rodents and monkeys, the entorhinal cortex interacts heavily with ventral/anterior hippocampus. We thus reasoned that olfactory information is most likely integrated with the anterior hippocampal pathways. To test this hypothesis, we divided hippocampal and parahippocampal regions into anterior (including perirhinal) and posterior (including retrosplenial) sections, and then computed connectivity between those sections and the primary olfactory cortical areas. A two-way repeated-measures ANOVA analysis with region (hippocampus vs. parahippocampus) and position (anterior vs. posterior) as independent variables revealed a main effect of position in the anterior olfactory nucleus ($F_{1,24}$ = 8.27, P = 0.0083; Fig. 2B), frontal piriform cortex ($F_{1,24}$ = 7.72, P = 0.010; Fig. 2D), and temporal piriform cortex ($F_{1,24}$ = 15.67, P = 0.00059; Fig. 2E). No main effect of position was found in the olfactory tubercle ($F_{1,24}$ = 0.19, P = 0.67; Fig. 2C). We found no main effect of region, nor interaction between region and position (all Ps > 0.05, Bonferroni corrected for multiple comparison of ANOVA analysis across seed ROIs). Post-hoc analyses using two-tailed paired t-tests revealed that all olfactory regions, with the exception of the olfactory tubercle, had stronger functional connectivity with the anterior aspect of both hippocampus and parahippocampus compared to the posterior aspects (P < 0.05, FDR corrected; Fig. 2B, D, E). This result suggests that, with the exception of the tubercle, there is preferential communication between primary olfactory cortices and the anterior hippocampal formation. Among primary olfactory cortical areas, the olfactory tubercle may possess a unique interface with the hippocampus, and in line with these findings, has been shown to exhibit connectivity with posterior aspects of the hippocampal formation (retrosplenial cortex) (Zhou et al., 2019a). Our finding that the connectivity pattern of the tubercle differs from other primary olfactory areas dovetails with a recent paper noting the multimodal functions of the olfactory tubercle, and suggesting it should more appropriately be called the tubular striatum (Wesson, 2020).

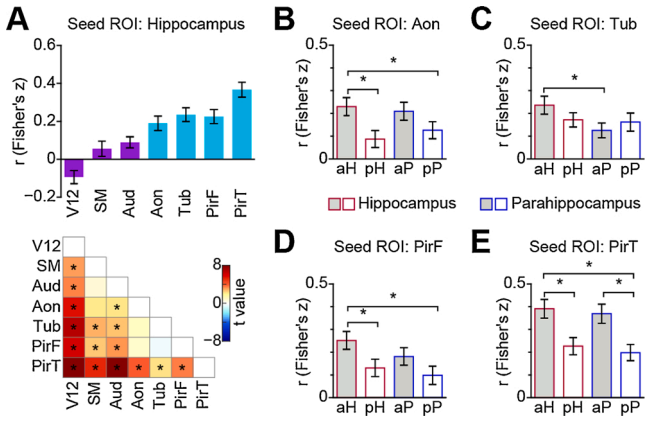

Fig. 2. Resting fMRI functional connectivity between hippocampus and primary olfactory subregions. (A). Hippocampal connectivity strength across sensory systems and primary olfactory subregions. Bar plot (top) indicates average correlation between seed and target region across participants (N = 25), light blue bars indicate olfactory cortical areas, dark purple bars indicate non-olfactory cortical areas. Error bars indicate standard error. T value map (bottom) was calculated using a two-tailed paired t-test. Asterisks indicate statistical significance (P < 0.05, FDR corrected). (B–E). Functional connectivity between olfactory cortical areas and anterior and posterior subregions of the hippocampal formation (hippocampus and parahippocampus); B: Anterior olfactory nucleus, C: Olfactory tubercle, D: Frontal piriform cortex, E: Temporal piriform cortex. Bar plots indicate the average correlation across participants (N = 25), and error bars indicate standard error. Asterisks indicate FDR corrected P < 0.05. Aon, anterior olfactory nucleus; Aud, Heschl's gyrus and planum temporale; PirF, frontal piriform cortex; PirT, temporal piriform cortex; SM, precentral and postcentral gyrus; Tub, olfactory tubercle; V12, V1 and V2; aH, anterior hippocampus; pH, posterior hippocampus; aP, anterior parahippocampus; pP, posterior parahippocampus.

2.2. Phase synchrony between piriform cortex and hippocampus

While fMRI provides whole-brain coverage, allowing direct comparison of hippocampal cortical networks across sensory systems, it has limited temporal resolution and does not provide a direct measure of neural activity. To examine human piriform-hippocampal connectivity at the neural level with high temporal precision, we recorded resting iEEG signals from eight participants undergoing invasive epilepsy evaluations. Each participant had between 6 and 14 electrode contacts implanted in the hippocampus (Fig. 3A, Table 1), and at least one

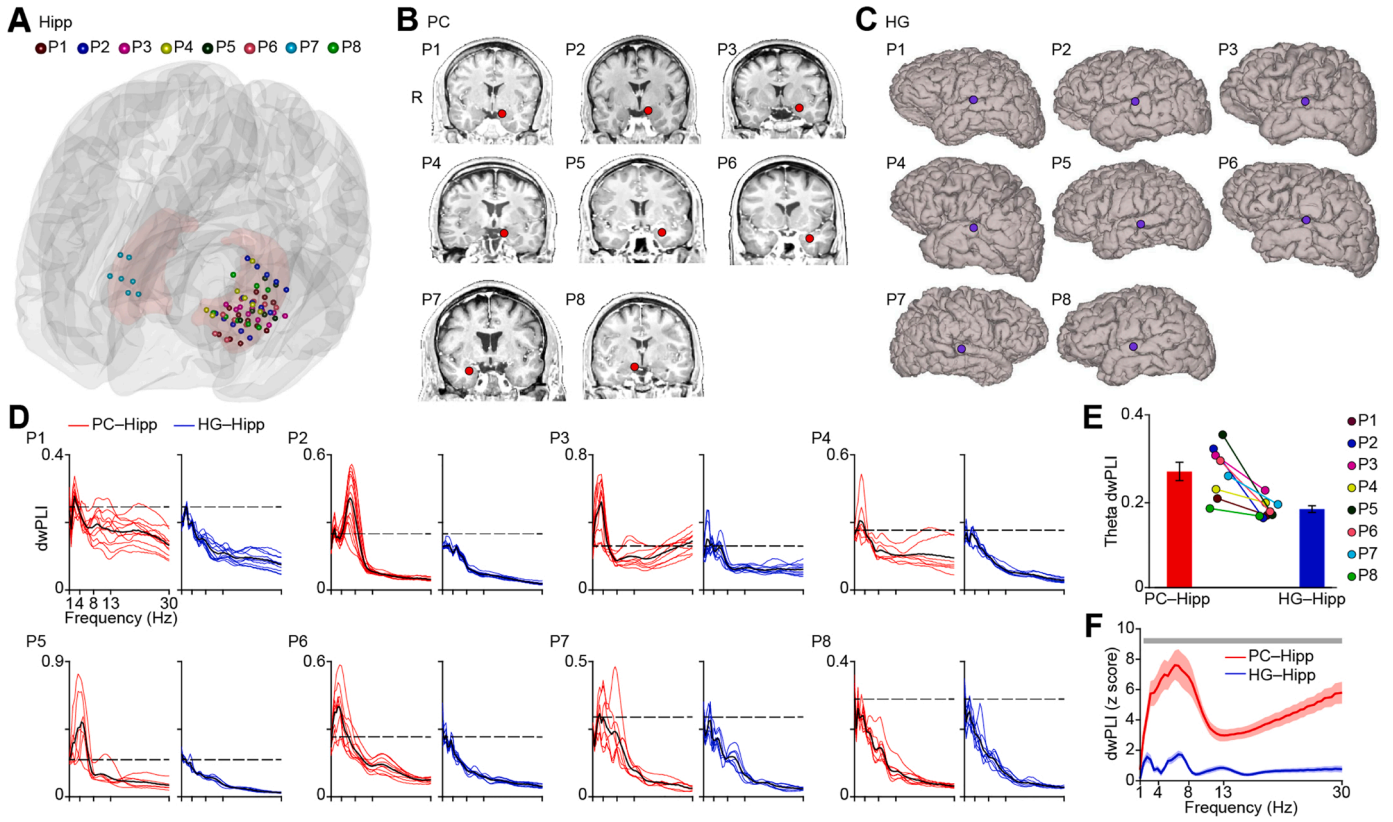

Fig. 3. Local field potential phase synchrony between piriform and hippocampus and between Heschl's gyrus and hippocampus. (A). Location of iEEG electrode contacts in hippocampus. Each color represents one participant, and each dot resents one electrode contact. The 3D model of the hippocampus (light red) is shown on a Montreal Neurological Institute standard brain. Dots represent electrode contact locations. Colors represent participants (P1–P8). (B). Location of iEEG electrode contacts (red dots) in the piriform cortex shown on each individual brain image for each participant (P1–P8). (C). Location of iEEG electrode contacts (blue dots) in auditory cortex shown on each individual brain surface for each participant (P1–P8). (D). Raw dwPLI for each participant (P1–P8) computed between piriform and hippocampus (red lines) and between auditory cortex and hippocampus (blue lines). The black solid lines indicate the average. The black dashed line indicates the significance threshold (95th percentile of the permuted dwPLIs, Bonferroni corrected) for each participant. (E). For each participant, theta-band phase synchrony between piriform and hippocampus is stronger than that between auditory cortex and hippocampus. Each colored dot represents one participant; bar plots represent the average over participants, and error bars indicate standard error. Differences between olfactory and auditory cortices were statistically significant (two-tailed paired *t*-test, $t_7 = 4.00$, $P = 0.0052$). (F). Phase synchrony between piriform and hippocampus (red line) is stronger than phase synchrony between auditory cortex and hippocampus (blue line) at each frequency. The solid line indicates the average over all electrode pairs across all participants (N = 72). The shaded area indicates standard error. Light gray bar indicates a statistically significant difference ($P < 0.05$, FDR corrected). R, right hemisphere; Hipp, hippocampus; HG, Heschl's gyrus; PC, piriform cortex.

Table 1
Demographic and clinical data of epilepsy patients.

Participant	Gender	Age at surgery (years)	Handedness	Duration of epilepsy (years)	Epileptogenic zone	Brain MRI	AED during day of task	Number of hippocampal contacts
P1	Male	32	Left	9	Left temporal lobe	Normal	None	11
P2	Male	47	Left	2	Left temporal lobe	Normal	None	14
P3	Female	29	Right	7	Left temporal lobe	Normal	None	10
P4	Male	49	Right	26	Left temporal lobe	Chronic stroke/encephalomalacia in left putamen, insula, parietal cortex	None	7
P5	Male	32	Right	10	Left basal temporal	Normal	Low dose	6
P6	Female	27	Right	5	Left mesial temporal	Left mesial temporal sclerosis	Low dose	9
P7	Male	54	Left	2	Right mesial temporal	Normal	None	7
P8	Female	25	Right	3	Left mesial temporal	Normal	None	8

electrode contact implanted in piriform cortex (Fig. 3B). All participants also had 1–2 contacts implanted in primary auditory cortex (Heschl's gyrus, according to FSL's Harvard-Oxford probability cortical atlas) (Fig. 3C), allowing us to compare olfactory-hippocampal phase synchrony with auditory-hippocampal phase synchrony. In our initial iEEG analyses, functional connectivity was computed over a broad frequency range (1–30 Hz in 0.25 Hz steps) using the debiased weighted Phase Lag Index (dwPLI), which is a robust measure of phase-based connectivity (phase locking) that is less sensitive to volume-conduction artifacts and common-source bias than other phase locking measures, such as Phase Locking Value (Stam et al., 2007; Vinck et al., 2011). To calculate the overall dwPLI between two regions, we first obtained analytic time series (Hilbert method) from each region of interest for each participant and segmented them into 5-second epochs. The dwPLI was calculated over time for each epoch and then averaged over epochs for each participant. We found significant phase locking (Fig. 3D, red lines; dashed line indicates 95th percentile of permuted dwPLIs, Bonferroni corrected for multiple participants) between piriform cortex and hippocampus in each participant in the lower frequency ranges, in agreement with our fMRI findings. However, significant phase locking was not consistently found between auditory cortex and hippocampus (Fig. 3D blue lines). Since phase locking was evidently maximal in the theta frequency range for most participants, we next conducted a direct statistical comparison between hippocampal connectivity of the two regions in the theta range. To this end, we calculated the average dwPLI in the theta (3–8 Hz) frequency range for all olfactory-hippocampal and auditory-hippocampal electrode pairs for each participant. Olfactory-hippocampal phase locking was stronger than auditory-hippocampal phase locking in the theta range for every participant (Fig. 3E, each dot is one value for each participant). This striking consistency in the results across participants was also reflected by a significant two-tailed paired *t*-test ($t_7 = 4.00$; $P = 0.0052$; Fig. 3E). Furthermore, in a combined analysis including all electrode pairs across all participants, a direct statistical comparison between the hippocampal connectivity of the primary olfactory and auditory cortices showed that olfactory cortex had significantly stronger connectivity with the hippocampus than did auditory cortex (permutation test; $P < 0.05$, FDR corrected; Fig. 3F; See **Materials and Methods**) in the 1.5–30 Hz frequency range, agreeing with our fMRI findings. Notably, group-level results showed an evident peak in the theta range, in agreement with our individual level results.

2.3. Olfactory-hippocampal connectivity oscillates with nasal breathing

Human and rodent studies suggest that olfactory cortical oscillations are impacted by respiratory phase (Fontanini et al., 2003; Fontanini and Bower, 2006, 2005; Liu et al., 2017; Lockmann et al., 2018; Masaoka et al., 2005; Tort et al., 2018; Tristan et al., 2009; Tsanov et al., 2014; Viczko et al., 2014; Zelano et al., 2016). Human and rodent studies also suggest that hippocampal oscillations are impacted by respiratory phase (human: Varga and Heck, 2017; Zelano et al., 2016; rodent: Heck et al., 2017; Herrero et al., 2018; Lockmann et al., 2018, 2016; Nguyen Chi et al., 2016; Yanovsky et al., 2014). Whether human olfactory-hippocampal networks are impacted by respiratory phase is, however, unknown. To test the hypothesis that resting human piriform-hippocampal connectivity varies over the respiratory cycle, we divided iEEG data into epochs aligned to inhale onsets (0.5 s before and 5 s after) and computed dwPLI across trials between the two regions.

We first conducted a combined, event-related analysis across all participants and electrode contacts. To account for differences in respiratory rate across participants, we normalized the dwPLI values by respiratory phase. The respiratory phase of each data point during inhale and exhale was obtained by linear interpolation between $-\pi$ (inhale onset) and 0 (exhale onset), and between 0 and π (exhale end), respectively (Fig. 4A), for each participant. The respiratory phase values were then divided into 200 equally-spaced bins and the dwPLI was averaged within each bin. The resulting plots of dwPLI over respiratory phase were pooled across all participants. This analysis was conducted for both piriform and auditory cortex. Significant dwPLI was evident over the entire respiratory period in the respiration-aligned event-related dwPLI map for piriform cortex ($P < 0.05$, FDR corrected; Fig. 4B top), but not at any phase of the respiratory period auditory cortex ($P > 0.05$, FDR corrected; Fig. 4B middle). A direct statistical comparison of hippocampal connectivity between regions showed stronger hippocampal dwPLI in piriform compared to auditory cortex over the entire respiratory period (permutation test; $P < 0.05$, FDR corrected; Fig. 4B bottom).

In piriform cortex, significant phase locking with the hippocampus was evident over the entire respiratory period (Fig. 4B top), limiting our ability to look for significant connectivity modulations induced by particular phases of respiration. Based on previous literature suggesting increased hippocampal oscillations during inhalation, we hypothesized

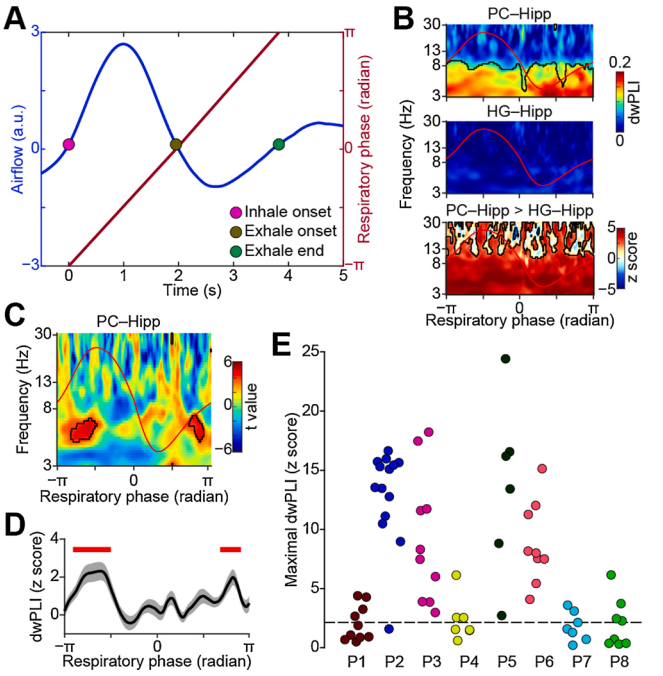

Fig. 4. Respiration modulates phase synchrony between piriform cortex and hippocampus. (A). Diagram illustrating linear interpolation of respiratory phase to account for differences in respiratory rate across participants. The blue line indicates respiratory signal and the red line indicates the corresponding respiratory phase. (B). Event-related phase synchrony between piriform cortex and hippocampus (top), between Heschl's gyrus and hippocampus (middle), and the difference between the two (bottom). Average respiration is overlaid (red line). Phase synchrony is significantly stronger between piriform and hippocampus over the entire respiratory period. Red areas with black outlines (bottom panel) indicate statistical significance ($P < 0.05$, FDR corrected). Note that black outlines blend with axes lines, as entire bottom area is significant.). (C). Inhale-induced increases in theta-band phase synchrony between the piriform cortex and hippocampus. Statistical comparison of pre- versus post- inhale phase locking across all electrode pairs and all participants (N = 72). Black outlines indicate a statistically significant increase in phase locking induced by inhalation ($P < 0.005$, FDR corrected). Average respiration is overlaid (red line). (D). Theta-band phase synchrony between the piriform cortex and hippocampus across the respiratory cycle. The solid black line indicates the average of normalized dwPLI (z score) over all electrode pairs (N = 72) in the theta frequency range. Shaded area indicates the standard error. Red bars indicate statistical significance (two-tailed one-sample *t*-test, $P < 0.005$, FDR corrected). (E). Maximal phase synchrony in each participant's piriform-hippocampus electrode pairs, in the significant cluster during inhale shown in panel C. The short-dashed line indicates the threshold of statistical significance ($P < 0.05$, FDR corrected). Each color represents one participant (P1–P8) and each dot represents one electrode pair. Hipp, hippocampus; HG, Heschl's gyrus; PC, piriform cortex; dwPLI, debiased weighted phase lag index.

that inhalation would drive increases in piriform-hippocampal phase locking. To better quantify changes associated with a particular phase of the respiratory cycle, we conducted a direct comparison between pre-inhale dwPLI values and post-inhale dwPLI values. First, we used the pre-inhale window (between 0.5 s and 0 s prior to inhale onset) as a baseline to examine inhale-induced dwPLI using a permutation method (see **Materials and Methods**). This resulted in a z score map for each piriform-hippocampus electrode pair. We then normalized the z score maps as a function of respiratory phase and examined the random effect of electrode pairs (N = 72) using a two-tailed one-sample *t*-test, resulting in a t value map of all electrode pairs. We found a significant increase in dwPLI just following inhalation, specifically in the theta frequency band (3–8 Hz) ($P < 0.005$, FDR corrected; Fig. 4C,D) in piriform cortex. This effect was evident both in the combined analysis across all participants (Fig. 4C), and at the individual level ($P < 0.05$, FDR corrected; Fig. 4E): Each participant had hippocampal contacts showing significant respiratory modulation of piriform-hippocampal connectivity ($P < 0.05$, FDR corrected; Fig. 4E).

2.4. Olfactory-hippocampal connectivity is not driven by distance or ROI size

In both fMRI and iEEG techniques, connectivity measures can be impacted by anatomical distance. In fMRI, vasculature may be more similar between nearby structures, thereby impacting functional connectivity measures (Tak et al., 2015), and in iEEG, volume conduction may produce artifactual connectivity between nearby structures (Kucyi et al., 2018). We therefore took measures to control for these potential confounds in our analyses. Our fMRI preprocessing steps included band-pass filtering at low frequency, motion-parameters regression, and global signal regression. Our iEEG analysis included dwPLI, which is designed specifically to reduce volume-conduction effects. However, to further validate that our findings were not due to volume conduction nor merely a reflection of distance from the hippocampus, we conducted several additional control analyses. First, we calculated the correlation between the distance from the hippocampus and connectivity strength, for both our fMRI and iEEG data sets. For the fMRI data, the ROIs included in our analyses were are made up of many voxels with variable anatomical distances to the hippocampus. Averaging over many voxels could have masked effects occurring more locally within larger ROIs. Therefore, we calculated the correlation between pairwise connectivity values for all voxels within all ROIs and their distance to the hippocampus. Our results showed that anatomical distance was not driving our connectivity analysis (Fig. 5A). Since olfactory cortex is closer to the hippocampus than other sensory cortices, proximity to the hippocampus could not explain our fMRI findings. For the iEEG data, we computed pairwise dwPLI of all electrode combinations within each participant, computed the distance between electrodes in each pair, and looked for a correlation between the two. We found no correlation between piriform-hippocampal connectivity and pairwise anatomical distance values. This was true for both the event-related (Spearman rho = 0.091, $P = 0.44$; Fig. 5C) and the overall dwPLI (Spearman rho = 0.058, $P = 0.63$; Fig. 5D) analyses. Since olfactory cortex is closer to the hippocampus than other sensory cortices, these data together suggest that proximity to the hippocampus did not drive our iEEG findings.

Next, we addressed the possibility that ROI size might have impacted the fMRI findings. Specifically, it is possible that larger ROIs could mask smaller subregions within them with strong hippocampal connectivity. To address this possibility, we re-computed the correlation between each target ROI and the hippocampus using a bootstrapping method (200 repetitions). For each bootstrap and ROI, a subset of contiguous voxels equal in number to the minimal number of voxels of any target ROI, was randomly extracted from each ROI without replacement. The correlations between the target ROI and the hippocampus were computed for each bootstrap, and the resulting correlations were averaged. Finally, we recomputed the one-way repeated-measures ANOVA

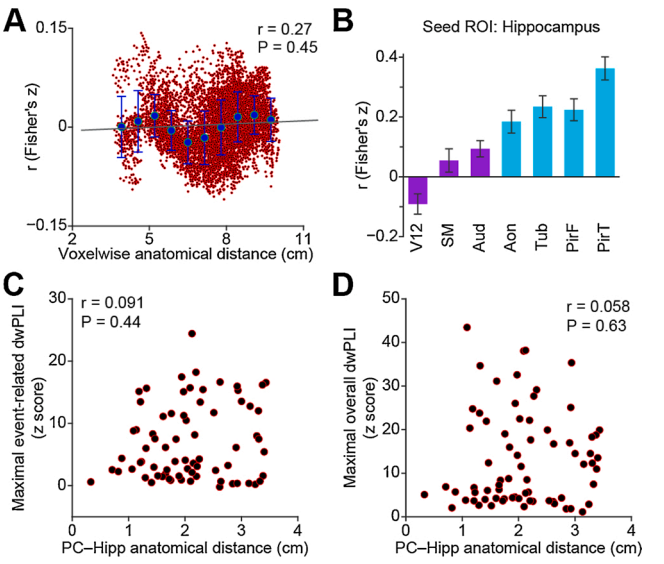

Fig. 5. Correlation between anatomical distance and functional connectivity. (A). Voxel-wise correlation between anatomical distance to the hippocampus and fMRI-based functional connectivity, across all voxels included in the analysis. Red dots indicate correlation values between distance and functional connectivity for all voxels. Blue dots indicate the average correlation values within each of ten equally distanced bins. Black line is the linear trend line. (B). Bootstrapped resting hippocampal fMRI connectivity strength across sensory systems. Bar plots are the average correlation across participants (N = 25). Light blue bars indicate olfactory cortical areas, dark purple bars indicate non-olfactory cortical areas. Error bars indicate standard error. (C). Spearman correlation between maximal event-related theta-band phase synchrony and anatomical distance between the piriform cortex and hippocampus. All piriform-hippocampus electrode pairs in all participants are shown (red dots). (D). Spearman correlation between maximal overall phase synchrony and anatomical distance between the piriform cortex and hippocampus. All piriform-hippocampus electrode pairs in all participants are shown (red dots). Aon, anterior olfactory nucleus; Aud, Heschl's gyrus and planum temporale; Hipp, hippocampus; PC, piriform cortex; V12, V1 and V2; SM, precentral and postcentral gyrus; PirF, frontal piriform cortex; PirT, temporal piriform cortex; Tub, olfactory tubercle, dwPLI, debiased weighted phase lag index.

analysis and found similar—in fact stronger—results compared to our original analysis ($F_{6,144} = 18.3$, $P = 1e{-}15$; Fig. 5B), suggesting that our findings were not driven by ROI size.

3. Discussion

Understanding principles of human brain function requires consideration of how sensory cortices engage cortical networks to support higher cognitive functions such as stimulus integration and memory encoding (Mesulam, 1998). Resting human hippocampal cortical networks are of particular interest because they are thought to have undergone evolutionary rerouting to pass through expanded association cortices before arriving at the hippocampus (Bergmann et al., 2016). These association cortices are assumed to enable more abstract stimulus representations and greater cognitive flexibility in humans compared to other mammals (Buckner and Krienen, 2013; Margulies et al., 2016). Previous work comparing rodent and human sensory-hippocampal networks focused on the visual, auditory and somatosensory systems, and found striking similarities between modalities (Sepulcre et al., 2012). However, the olfactory system, which was not considered, differs from other sensory systems both in organization and in evolution (Vermetten and Bremner, 2003). Our results, which agree with recent human evoked-potential findings (Skopin et al., 2020), show that unlike other sensory systems, human hippocampal networks include primary olfactory cortices, suggesting that the proposed evolutionary rerouting

of hippocampal networks did not include the olfactory system. This supports the notion that human olfactory-hippocampal networks remain similar to those found in rodents (Goulas et al., 2019).

Our results are of relevance for cognitive psychology as there is a long-standing hypothesis that memories involving odors are shaped by unique hippocampal interactions with the olfactory system (Herz and Engen, 1996; Plailly et al., 2019; Saive et al., 2015, 2014; White, 1998; Zucco, 2003). Previous studies have shown that declarative memory processes—those related to knowledge and episodes, and consciously accessible—involve the hippocampus (see Eichenbaum, 2000; Squire and Zola, 1996 for reviews). Importantly, such declarative memory processes appear different for odors than for visual and auditory stimuli. For example, odor-elicited autobiographical memories are more vivid and more often involve events experienced in childhood than memories elicited by other stimuli (Chu and Downes, 2000; Cornell Kärnekull et al., 2020; Willander and Larsson, 2006). Episodic odor memories are, furthermore, characterized by an unusually low level of forgetting over time (Cornell Karnekull et al., 2015; Lawless, 1978). These results seemingly provide credence to the oft-referenced notion described by Marcel Proust that "*But when from a long-distant past nothing subsists, after the people are dead … taste and smell alone … remain poised a long time … and bear unflinchingly, in the tiny and almost impalpable drop of their essence, the vast structure of recollection*" (Proust, 1922). Interestingly, initial odor-object associations may retain a privileged mnemonic status because of an unusually high hippocampal engagement relative to sound-object associations (Yeshurun et al., 2009), and autobiographical memories evoked by odors engage the hippocampus to a high degree (Arshamian et al., 2013; Herz et al., 2004). However, it should be noted that such olfactory advantages maybe counteracted by relatively high false-alarm rates (Cornell Karnekull et al., 2015), such that overall performance on memory tasks can be lower for odors than for faces, words, and other stimuli. Olfaction is also limited in knowledge-based memory capacity relative to some other senses (Cain, 1979; Herz and von Clef, 2001). In sum, unique olfactory interactions with the hippocampus may affect olfactory-based memory processes in several ways. The present study does not include an assessment of odor processing or anatomical projections. However, our results may have important implications for the field of olfactory-based memory. First, our results suggest that hippocampal connectivity with primary and secondary cortices might be fruitfully employed in fMRI assessments of cross-modal memory processes (e.g., similar to Gottfried and Dolan, 2003), in order to study the functional relevance of such connections. Second, our results support the notion that input from primary olfactory cortices reaches the hippocampus via direct projections, hence presenting olfactory information to the hippocampus in a less processed form than input from other senses. It was previously proposed that olfaction has direct access to integrative language hubs such as the temporal pole (Olofsson et al., 2013; Zhou et al., 2019a), and that this might explain the difficulty in verbalizing familiar odors, as they do not receive adequate perceptual processing prior to cognitive integration (Olofsson and Gottfried, 2015). Future work should address whether the observed preferential hippocampal connectivity with primary olfactory cortices may be credibly invoked to explain the vividness, accuracy, longevity, or other memory-related features of odors relative to other stimuli.

The presumed evolutionary preservation of human olfactory-hippocampal networks suggests that rodent olfactory-hippocampal networks function as an excellent model for human (Eichenbaum et al., 1994; Eichenbaum and Robitsek, 2009; Gewirtz et al., 2000; Hasselmo and McClelland, 1999; Levinson et al., 2020; McNish et al., 2000; Otto et al., 1991b, 1991a; Sullivan et al., 2015). While a direct comparison between human and rodent olfactory-hippocampal networks is beyond the scope of this manuscript, our findings support the idea that some properties of human olfactory memory networks may be inferred from rodents (Alvarez, 2002; Aqrabawi and Kim, 2020; Heck et al., 2019; Kay, 2014; Komiyama and Luo, 2006; Martin et al., 2007; Martin and Ravel, 2014; McNamara et al., 2008; Staubli et al., 1986; Sullivan, 2003; Veyrac et al., 2015; Wilson et al., 1986). Olfactory functioning provides a useful tool for assessing mild cognitive impairment and amnestic dementia (Conti et al., 2013; Devanand et al., 2020; Doty and Hawkes, 2019; Hummel et al., 2009; Murphy, 2019; Stanciu et al., 2014). Similarities between human and rodent olfactory networks during memory tasks might suggest a high level of cross-species translation, which could be useful for clinical studies (Meunier et al., 2014; Moss et al., 2019; Olofsson et al., 2019; Zhou et al., 2019b).

The olfactory system is inextricably tied to breathing. We found that connectivity between human piriform cortex and the hippocampus was modulated over the respiratory cycle, in the absence of an olfactory task. This suggests that even in unattended, restful states, primary olfactory cortex is dynamically communicating with the hippocampus (Arshamian et al., 2018). These data directly support the fundamental idea that respiratory rhythms function as an organizational unit of olfactory networks in humans, which has been previously shown in rodents (Biskamp et al., 2017; Buonviso et al., 2003; Liu et al., 2017; Lockmann et al., 2018, 2016; Lockmann and Tort, 2018; Nguyen Chi et al., 2016; Yanovsky et al., 2014). Notably, we found phase locking of piriform and hippocampal oscillations in the theta frequency band, which has strong ties to respiration in rodents (Kay, 2005; Rojas-Líbano et al., 2014), so much so that rodent theta oscillations are often referred to as "respiratory oscillations" (Fontanini et al., 2003; Heck et al., 2019; Kay et al., 2009; Kay and Stopfer, 2006). Rodent respiratory rhythms overlap with the theta frequency band, unlike humans who breath much more slowly (~0.1 to 0.3 Hz). Interestingly, despite dramatic differences in respiratory rates across species, theta oscillations are rhythmic with respiratory rhythms in both species. In humans, unattended, natural breathing of clean (non-odorized) air may still activate olfactory receptors in the nose (Sobel et al., 1998b), and could potentially activate piriform cortex as well (Bensafi et al., 2007; Kareken et al., 2004; Koritnik et al., 2009; Sobel et al., 1998a; Zelano et al., 2016). Previous research shows that sniffing drives cortical activity in the piriform cortex and supports olfactory perception in several ways (see Mainland and Sobel, 2006 for review). Sniffing is also linked to odor memory consolidation as well as the recollection of familiar household odors (Arshamian et al., 2018, 2008; Bensafi et al., 2013). Future work may address how sniffing affects hippocampal-olfactory networks to potentially achieve olfactory-cognitive processes.

A fair question is whether this mechanical activation of olfactory receptors during natural breathing explains the increased functional connectivity between olfactory cortex and the hippocampus compared to other sensory systems. We think this is unlikely for several reasons. First, olfactory connectivity exceeded auditory connectivity not only during inhalation, but over the entire respiratory period. Our iEEG data show that higher functional connectivity with the hippocampus was present for piriform compared to auditory cortex throughout the respiratory cycle. Furthermore, sounds and physical sensations of the fMRI pulse sequence were also present during scanning, presumably driving auditory and somatosensory primary cortices. But this was not enough to increase their hippocampal connectivity beyond that of primary olfactory cortex. Thus, inhalation-induced activation of olfactory cortex is unlikely to explain our findings.

Our findings are in line with the notion that the olfactory system is unique amoung sensory systems, in terms of both its evolutionary status and its anatomical organization (Ennis et al., 2015). That said, the olfactory system is less understood than other modalities (Gottfried, 2010), and the specific functions of primary olfactory cortical areas in olfactory processing are far from clear (Bensafi et al., 2007; Gottfried et al., 2006, 2004, 2002; Howard et al., 2009; Li et al., 2008, 2006; Sobel et al., 2000, 1999; Zelano et al., 2005). Historically, primary olfactory cortex has been defined to include all brain areas that receive direct monosynaptic input from the olfactory bulb (Allison, 1954; Carmichael et al., 1994; Feher, 2017; Gottfried, 2010; Mai and Paxinos, 2012; Price, 2009). More recently, however, this definition has been challenged, as

piriform cortex may perform associative functions in olfactory processing (Calu et al., 2007; Chen et al., 2014; Choi et al., 2011; Gire et al., 2013; Gottfried and Dolan, 2003; Johnson et al., 2000; Karunanayaka et al., 2015; Martin et al., 2006; Pashkovski et al., 2020; Roesch et al., 2006; Sacco and Sacchetti, 2010; Schoenbaum and Eichenbaum, 1995) in addition to basic coding of odor identity and chemical features (Howard et al., 2009; Kadohisa and Wilson, 2006; Pashkovski et al., 2020; Roland et al., 2017). Therefore, an intriguing interpretation of our findings is that olfactory associative cortex includes piriform cortex, thereby eliminating the need for rerouting of hippocampal networks. However, it is worth noting that we found stronger connectivity relative to other sensory cortices between the hippocampus and other primary olfactory cortices as well, including the anterior olfactory nucleus and the olfactory tubercle. Furthermore, higher order functions such as attention and multi-sensory integration have been ascribed to primary sensory cortices in the visual and auditory systems as well (Galambos et al., 1956; Lakatos et al., 2007; Lee et al., 2002, 1998; Meredith and Allman, 2015; Rauschecker, 1999; Schroeder et al., 2004), supporting the validity of our comparison of primary sensory cortices across modalities.

In summary, our findings show unique properties of human olfactory-hippocampal networks relative to other sensory modalities. Similar to the rodent brain, but unlike other human sensory systems, the human olfactory system maintained functional connectivity with the hippocampus. Our results might stimulate further research that will specify the detailed anatomical properties of human olfactory-hippocampal networks, assess their presumed roles in shaping olfactory memory experiences, and explore their translational potential in the field of neurodegenerative disorders.

4. Materials and methods

4.1. Resting-state fMRI experiment

For the rsfMRI study, we used an existing data set that has been previously described (Zhou et al., 2019a). Twenty-five healthy participants (mean ± standard error age: 25.5 ± 1.2 years; 14 women) completed a 10-minute eyes-open rsfMRI scan using a single-shot gradient-echo planar-imaging sequence with following parameters: repetition time (TR) = 555 ms; echo time (TE) = 22 ms; flip angle = 47°; field of view (FOV) = 208 mm; voxel size = $2 \times 2 \times 2$ mm^3; 64 axial slices. All participants gave written informed consent and all methods were approved by the Institutional Review Board of Northwestern University. Participants were asked to breathe naturally through their noses. A high-resolution T1-weighted MPRAGE anatomical image was also acquired for each participant (TR = 2300 ms; TE = 2.94 ms; flip angle = 9°; FOV = 256 mm; voxel size = $1 \times 1 \times 1$ mm^3; 176 sagittal slices). MRI data were collected on a 3 T Siemens TIM Trio MRI scanner (Siemens Healthcare, Erlangen, Germany) at the Northwestern University Center for Translational Imaging (https://cti.northwestern.edu).

4.2. iEEG experiment

Eight epilepsy patients (3 women) who were undergoing surgical seizure monitoring at Northwestern Memorial Hospital participated in this study. Participant demographic data are shown in Table 1. All participants gave written informed consent and all methods were approved by the Institutional Review Board of Northwestern University. The clinically-planned electrode placement scheme for all participants provided coverage of the piriform cortex, auditory cortex and hippocampus. Electrode placement and respiratory monitoring techniques did not deviate from standard clinical procedures at Northwestern Memorial Hospital.

Participants were instructed to sit comfortably breathing through their noses with their eyes open for 15 min while iEEG data were recorded using a clinical Nihon Kohden acquisition system. For two of the eight participants, only 5 min of data were available. The sampling rate, which was determined clinically, ranged from 1000 Hz to 2000 Hz across participants. A surgically implanted electrode strip facing towards the scalp served as the reference and ground. Respiratory signals were recorded using a spirometer with a piezoelectric pressure transducer (Salter Labs Model # 5500) attached to a nasal cannula placed at the participant's nose, and a breathing belt placed around the participant's abdomen. We used the spirometer signal in our analysis in all participants except for two, on whom spirometer recordings were not obtained.

4.3. fMRI data analysis

The preprocessing of rsfMRI data was performed using FSL's FEAT (FMRIB Software Library, www.fmrib.ox.ac.uk/fsl, version 5.0.10) (RRID:SCR_002823) (Jenkinson et al., 2012; Smith et al., 2004; Woolrich et al., 2009) and included: 1) removal of the first 10 volumes; 2) motion correction; 3) spatial registration with default options. Next, we removed the linear and quadratic trends using Analysis of Functional NeuroImages (AFNI) (RRID:SCR_005927) (Courtiol and Wilson, 2015) and regressed out nuisance variables—including 6 head-movement parameters, and global whole brain, white matter and cerebrospinal signals—using multiple linear regression (FSL's *fsl_glm*). The global signal regression method we used is effective for controlling physiological artifacts, including respiration, in fMRI functional connectivity analysis (Weiss et al., 2020). To create the white matter and cerebrospinal masks, we extracted the brain from the structural image and segmented it into gray matter, white matter and cerebrospinal fluid using FSL's BET (Smith, 2002) and FAST (Zhang et al., 2001) tools. The resulting white matter and cerebrospinal fluid images were further eroded by 1 voxel (FSL's *fslmaths*). Finally, the preprocessed fMRI images were intensity normalized, band-pass filtered (0.008–0.1 Hz, AFNI's *3dFourier*), registered to MNI space and spatially smoothed (Gaussian kernel, sigma = 3).

To examine the correlation between the hippocampus and visual, auditory, somatosensory, and olfactory cortices, we outlined ROIs for each brain area. For anterior and posterior hippocampus, the hippocampus atlas that is included in FSL (HarvardOxford-sub-maxprob-thr50−2 mm) was used, with y = −20 mm (Poppenk et al., 2013). For early visual areas, including primary and secondary visual cortex, we used *Freesurfer* (cvs_avg35_inMNI152, http://surfer.nmr.mgh.harvard.edu/) (Hinds et al., 2008). For primary auditory cortex (Heschl's gyrus and planum temporale) and somatosensory (precentral and postcentral gyrus) cortices, we used the Harvard-Oxford atlas (HarvardOxford-sub-maxprob-thr50−2 mm and HarvardOxford-cort-maxprob-thr50−2 mm). ROIs of the olfactory cortical regions were drawn manually on a MNI standard brain according to previously published work (Mai et al., 2015; Zhou et al., 2019a). Finally, the HarvardOxford-cort-maxprob-thr50−2 mm was used for the anterior and posterior parahippocampus. The time series of all voxels within each ROI were extracted and averaged. The correlation between the hippocampus and the ROIs was calculated using Pearson correlation coefficient (Fisher z-transformation).

To compare functional connectivity between the hippocampus and piriform cortex to that between the hippocampus and other primary sensory cortices, we performed a two-way repeated-measures ANOVA analysis (factor hemisphere: left and right hemisphere. factor region: primary visual (V1 and V2), auditory (A1 and A2), somatosensory (S1) and olfactory cortices) for left and right hippocampus seed ROIs separately. Post-hoc tests were performed using two-tailed paired *t*-tests and multiple comparisons were corrected for using FDR (Benjamini and Hochberg, 1995). All *P* values reported in this paper were two-tailed unless stated otherwise.

To compare functional connectivity between the hippocampus and additional primary olfactory regions, we manually drew ROIs of the anterior olfactory nucleus and the olfactory tubercle on the MNI brain according to the human brain atlas (Mai et al., 2015; Zhou et al., 2019a). The piriform cortex was also divided into frontal and temporal

subregions, as outlined in the atlas. Then, we used a one-way repeated-measures ANOVA analysis (factor region) for the hippocampus seed ROI. Post-hoc tests were performed using two-tailed paired *t*-tests and multiple comparisons were corrected for using FDR. In this analysis, we combined the left and right hemispheres by averaging the fMRI time series for both the seed and target ROIs before calculating the correlation between the hippocampus and the olfactory cortices.

To examine functional connectivity between olfactory regions and anterior and posterior sections of the hippocampal formation (hippocampus and parahippocampus), we performed a two-way repeated-measures ANOVA analysis for each olfactory region with the region (hippocampus vs. parahippocampus) and position (anterior vs. posterior) as independent variables. Post-hoc analyses were performed using two-tailed paired *t*-tests and multiple comparisons were corrected for using FDR.

To examine the effect of ROI size on our findings, we performed an additional bootstrapping analysis. In each bootstrap, we extracted the average time series from a subset of contiguous voxels, equal in number to the minimal number of voxels of any target ROI, for each target ROI (left and right hemispheres merged). We then calculated the correlation between the hippocampus and target ROIs, and performed a one-way repeated-measures ANOVA analysis (factor: region) on the correlation matrix. Post-hoc analyses were performed using two-tailed paired *t*-tests and multiple comparisons were corrected for using FDR.

To examine the relationship between functional connectivity and anatomical distance, we calculated the functional connectivity and Euclidian distance of every pair of voxels between the hippocampus and target ROIs. This analysis resulted a connectivity and distance matrix where the rows and columns correspond to the voxels in the hippocampus and target ROIs respectively. Then, we averaged both the connectivity and distance matrices over all hippocampal voxels. Next, we divided the anatomical distance into 10 equally-spaced bins and calculated the average connectivity within each bin. Finally, the correlation between the connectivity and anatomical distance was examined using Spearman correlation.

4.4. iEEG data analysis

iEEG and respiratory data were down-sampled to 500 Hz using Matlab (RRID:SCR_001622; The MathWorks Inc., Natick, Massachusetts) toolbox *fieldtrip* (RRID:SCR_004849) (Oostenveld et al., 2011). Power line noise (60 Hz and its harmonics) was removed from the iEEG data using notch filters. To minimize any contribution of global oscillations to our signal, the resulting data were re-reference to the common average. Respiratory signals were further low-pass filtered at 3 Hz and z-score normalized. Low-pass/band-pass filtering of the respiratory signal and iEEG data was performed using a finite impulse response filter as implemented in *fieldtrip*. Then, the inhale onset of each breath across the acquisition was estimated using BreathMetrics (Noto et al., 2018).

To determine the electrode locations, the post-operative computed tomography images were registered to individual pre-operative structural MRI images using FSL's linear registration tool. The transformed post-operative computed tomography images were thresholded and each electrode was identified manually. We used the center of each identified electrode as its coordinate in individual anatomical space. In order to visually represent electrodes across participants in one image, electrode coordinates were converted into MNI space by normalizing individual MRI images to a standard MNI brain (MNI152_1mm_brain). We also performed subcortical segmentation of each individual's MRI image using *Freesurfer* (RRID:SCR_001847); any electrode that was labeled as the hippocampus by either *Freesurfer*'s segmentation or FSL's atlas (Harvard-Oxford subcortical atlas) was included in our analysis (Table 1). A single piriform cortex contact was identified on each individual brain image based on the human brain atlas (Mai et al., 2015). Finally, a single Heschl's gyrus contact was identified based on the Harvard-Oxford cortical atlas.

To examine overall phase coupling between piriform cortex and hippocampus and that between primary auditory cortex and hippocampus, we calculated dwPLI (Vinck et al., 2011) between both piriform cortex and Heschl's gyrus, and the hippocampus. The data were band-pass filtered from 1 to 30 Hz in steps of 0.25 Hz (bandwidth: 2 Hz). Then, the analytic time series were obtained using the Hilbert transform method, and segmented into 5 s epochs. The dwPLI was calculated over time for each epoch and the resulting dwPLIs were averaged over all epochs for each electrode pair and participant.

To estimate the statistical significance of the dwPLI, we used a permutation method. For each permutation, the epoch labels were shuffled for one of the two channels before calculating the phase difference between those two channels. Then, the dwPLI was calculated as described above. The permutation procedure (10,000 repetitions) was performed for piriform cortex–hippocampus and Heschl's gyrus–hippocampus electrode pairs separately for each participant. We used a Monte Carlo method for the permutation test, i.e., the hippocampal electrode was randomly selected from all hippocampal electrodes in each permutation. To derive a single dwPLI significance threshold for each participant, we pooled the permuted dwPLI values across all frequencies of both piriform cortex–hippocampus and Heschl's gyrus–hippocampus electrode pairs. Then, we calculated the 99.375th percentile, which corresponds to a P value of 0.05 (Bonferroni correction across participants), of the distribution of combined permuted dwPLI values. To compare the dwPLI between piriform cortex–hippocampus and Heschl's gyrus–hippocampus, we calculated the mean dwPLI within the theta frequency range (3–8 Hz) of both piriform cortex–hippocampus and Heschl's gyrus-hippocampus electrode pairs for each participant. Then, we used a two-tailed paired *t*-test to compare the dwPLI values between the piriform cortex and hippocampus to those between the Heschl's gyrus and hippocampus across participants ($N = 8$). Note, a z score was calculated for the real dwPLI at each frequency. To do so, the mean and standard deviation of the null distribution of each frequency was calculated using Matlab's *normfit*. The z score was then calculated by subtracting the mean of the null distribution, which was further divided by its standard deviation.

We further compared the coupling between piriform cortex and hippocampus to that between the Heschl's gyrus and hippocampus at each frequency using a permutation test. In each permutation, the labels of each electrode pair were switched randomly, and the difference of the normalized dwPLI between the two conditions was calculated. We repeated this procedure 10,000 times to obtain a null distribution of differences at each frequency. Then, a z score of the real difference was tested against this assumed normal null distribution. Multiple comparisons across frequency were corrected using FDR. Note, we pooled all electrode pairs across participants, resulting in seventy-two piriform cortex–hippocampus electrode pairs and seventy-two Heschl's gyrus–hippocampus electrode pairs that were used in the permutation analysis.

To examine whether phase coupling between piriform cortex and hippocampus varied over the respiratory cycle, we calculated event-related dwPLI across epochs that were aligned to inhale onsets (0.5 s before to 5 s after inhale onset). The center frequency of the previously applied bandpass filter ranged between 3 Hz and 30 Hz (50 log-spaced frequencies, based on group-level dwPLI showing maximal values beginning at 3 Hz) and the bandwidth was set at 2 Hz. To account for differences in respiratory frequency across participants, we normalized the dwPLI as a function of respiratory phase for each participant. To do so, the respiratory signal was segmented and averaged over all epochs. Each trial was baseline-corrected by subtracting the average of a 100 ms pre-inhale-onset time window. We then defined the first, second and third zero-cross points of the averaged respiratory signal as inhale onset, exhale onset and exhale end respectively. The respiratory phase at each data point during inhale and exhale was calculated by linear interpolation between $-\pi$ and 0, and between 0 and π respectively (Fig. 4A). The respiratory phase was then divided into 200 equally-spaced bins,

and the average dwPLI was calculated for each bin. We used a permutation test (1000 permutations) to evaluate the significance of the raw event-related dwPLI. In each permutation, the trial label of the hippocampal channel was randomly shuffled before the dwPLI was calculated. The dwPLI was averaged over all electrode pairs, resulting a null distribution of dwPLI at each respiratory phase-frequency point. The average and standard deviation of the null distribution was calculated by a normal fitting method. Finally, a z score was calculated by subtracting the average of the null distribution from the real dwPLI, which was further divided by the standard deviation of the distribution.

To compare event-related dwPLI between piriform and hippocampus to that between Heschl's gyrus and hippocampus, we used a similar permutation test. In each permutation, the labels of each electrode pair were switched randomly and the difference of event-related dwPLI between the two conditions was calculated. We repeated this 10,000 times to get a null distribution of the difference at each frequency and respiratory phase point. Then, a z score of the real difference at each frequency and respiratory phase was tested against this assumed normal null distribution. Multiple comparisons were corrected using the FDR method.

To further account for the difference in the number of respiratory cycles across participants, we z score normalized the dwPLI map to the pre-inhale time window ([−0.5, 0] s prior to inhale onset) using the trial shuffling permutation method as described above. In each permutation, the mean of the baseline dwPLI was subtracted from the raw permuted dwPLI. A repetition of 1000 permutations resulted in a null distribution of dwPLI change at each time-frequency point. Then, a z score of the real dwPLI change was calculated by subtracting the average of the null distribution from the real dwPLI, which was further divided by the standard deviation of the distribution. Finally, the resulting z score map was normalized as function of respiratory phase. Random effects of the normalized dwPLI at each frequency and each respiratory phase bin were tested using a two-sided one-sample *t*-test over all electrode pairs ($N = 72$). Multiple comparisons across frequencies and phase bins were corrected using FDR.

To examine the spatial distribution of the dwPLI, the maximal event-related dwPLI of the statistically significant cluster during inhale in the theta frequency range was computed for each electrode pair. The maximal overall dwPLI was also calculated in the low frequency range (< 8 Hz). The anatomical distance between the piriform cortex and the hippocampus electrodes was calculated as the Euclidian distance between these two electrodes. Finally, we used Spearman correlation to examine the relationship between the dwPLI and anatomical distance.

Declaration of Competing Interest

The authors report no declarations of interest.

Acknowledgments

We thank Enelsa Lopez and Navid Shadlou for their technical support and assistance with data collection. This work was supported by National Institutes of Health grants R00-DC-012803(NIDCD) and R01-DC-016364(NIDCD) to C. Z., and R01-NS-113804(NINDS) to J.V. and by grants from the Knut and Alice Wallenberg Foundation (KAW 2016:0229) and the Swedish Research Council (2020-00266) to J.K.O.

Appendix A. The Peer Review Overview and Supplementary data

The Peer Review Overview and Supplementary data associated with this article can be found in the online version, at doi: https://doi.org/10.1016/j.pneurobio.2021.102027.

References

Allen, T.A., Fortin, N.J., 2013. The evolution of episodic memory. Proc. Natl. Acad. Sci. U. S. A. 110, 10379–10386. https://doi.org/10.1073/pnas.1301199110.

Allison, A.C., 1954. The secondary olfactory areas in the human brain. J. Anat. 88, 481–488.

Alvarez, P., 2002. Hippocampal formation lesions impair performance in an odor-odor association task independently of spatial context. Neurobiol. Learn. Mem. 78, 470–476. https://doi.org/10.1006/nlme.2002.4068.

Aqrabawi, A.J., Kim, J.C., 2020. Olfactory memory representations are stored in the anterior olfactory nucleus. Nat. Commun. 11, 1246. https://doi.org/10.1038/s41467-020-15032-2.

Arnold, T.C., You, Y., Ding, M., Zuo, X.-N., de Araujo, I., Li, W., 2020. Functional connectome analyses reveal the human olfactory network organization. eneuro 7. ENEURO. https://doi.org/10.1523/ENEURO.0551-19.2020, 0551-19.2020.

Aronoff, R., Matyas, F., Mateo, C., Ciron, C., Schneider, B., Petersen, C.C.H., 2010. Long-range connectivity of mouse primary somatosensory barrel cortex. Eur. J. Neurosci. 31, 2221–2233. https://doi.org/10.1111/j.1460-9568.2010.07264.x.

Arshamian, A., Olofsson, J.K., Jönsson, F.U., Larsson, M., 2008. Sniff your way to clarity: the case of olfactory imagery. Chemosens. Percept. 1, 242–246. https://doi.org/10.1007/s12078-008-9035-z.

Arshamian, A., Iannilli, E., Gerber, J.C., Willander, J., Persson, J., Seo, H.S., Hummel, T., Larsson, M., 2013. The functional neuroanatomy of odor evoked autobiographical memories cued by odors and words. Neuropsychologia 51, 123–131. https://doi.org/10.1016/j.neuropsychologia.2012.10.023.

Arshamian, A., Iravani, B., Majid, A., Lundström, J.N., 2018. Respiration modulates olfactory memory consolidation in humans. J. Neurosci. 38, 10286–10294. https://doi.org/10.1523/JNEUROSCI.3360-17.2018.

Banks, S.J., Sreenivasan, K.R., Weintraub, D.M., Baldock, D., Noback, M., Pierce, M.E., Frasnelli, J., James, J., Beall, E., Zhuang, X., Cordes, D., Leger, G.C., 2016. Structural and functional MRI differences in master sommeliers: a pilot study on expertise in the brain. Front. Hum. Neurosci. 10, 414. https://doi.org/10.3389/fnhum.2016.00414.

Barkai, E., Saar, D., 2001. Cellular correlates of olfactory learning in the rat piriform cortex. Rev. Neurosci. 12, 111–120. https://doi.org/10.1515/REVNEURO.2001.12.2.111.

Benjamini, Y., Hochberg, Y., 1995. Controlling the false discovery rate: a practical and powerful approach to multiple testing. J. R. Stat. Soc. Ser. B 57, 289–300. https://doi.org/10.1111/j.2517-6161.1995.tb02031.x.

Bensafi, M., Sobel, N., Khan, R.M., 2007. Hedonic-specific activity in piriform cortex during odor imagery mimics that during odor perception. J. Neurophysiol. 98, 3254–3262. https://doi.org/10.1152/jn.00349.2007.

Bensafi, M., Iannilli, E., Schriever, V.A., Poncelet, J., Seo, H.-S., Gerber, J., Rouby, C., Hummel, T., 2013. Cross-modal integration of emotions in the chemical senses. Front. Hum. Neurosci. 7, 883. https://doi.org/10.3389/fnhum.2013.00883.

Bergmann, E., Zur, G., Bershadsky, G., Kahn, I., 2016. The organization of mouse and human cortico-hippocampal networks estimated by intrinsic functional connectivity. Cereb. Cortex 26, 4497–4512. https://doi.org/10.1093/cercor/bhw327.

Biskamp, J., Bartos, M., Sauer, J.-F., 2017. Organization of prefrontal network activity by respiration-related oscillations. Sci. Rep. 7, 45508. https://doi.org/10.1038/srep45508.

Buckley, M.J., Gaffan, D., 1997. Impairment of visual object-discrimination learning after perirhinal cortex ablation. Behav. Neurosci. 111, 467–475. https://doi.org/10.1037/0735-7044.111.3.467.

Buckner, R.L., Krienen, F.M., 2013. The evolution of distributed association networks in the human brain. Trends Cogn. Sci. 17, 648–665. https://doi.org/10.1016/j.tics.2013.09.017.

Buonviso, N., Amat, C., Litaudon, P., Roux, S., Royet, J.-P., Farget, V., Sicard, G., 2003. Rhythm sequence through the olfactory bulb layers during the time window of a respiratory cycle. Eur. J. Neurosci. 17, 1811–1819. https://doi.org/10.1046/j.1460-9568.2003.02619.x.

Burwell, R.D., 2006. The parahippocampal region: corticocortical connectivity. Ann. N. Y. Acad. Sci. 911, 25–42. https://doi.org/10.1111/j.1749-6632.2000.tb06717.x.

Burwell, R.D., Amaral, D.G., 1998. Perirhinal and postrhinal cortices of the rat: interconnectivity and connections with the entorhinal cortex. J. Comp. Neurol. 391, 293–321. https://doi.org/10.1002/(SICI)1096-9861(19980216)391:3<293::AID-CNE2>3.0.CO;2-X.

Cabral, J., Kringelbach, M.L., Deco, G., 2014. Exploring the network dynamics underlying brain activity during rest. Prog. Neurobiol. 114, 102–131. https://doi.org/10.1016/j.pneurobio.2013.12.005.

Cain, W., 1979. To know with the nose: keys to odor identification. Science (80-.) 203, 467–470. https://doi.org/10.1126/science.760202.

Calu, D.J., Roesch, M.R., Stalnaker, T.A., Schoenbaum, G., 2007. Associative encoding in posterior piriform cortex during odor discrimination and reversal learning. Cereb. Cortex 17, 1342–1349. https://doi.org/10.1093/cercor/bhl045.

Carey, R.M., Wachowiak, M., 2011. Effect of sniffing on the temporal structure of mitral/tufted cell output from the olfactory bulb. J. Neurosci. 31, 10615–10626. https://doi.org/10.1523/JNEUROSCI.1805-11.2011.

Carmichael, S.T., Clugnet, M.-C., Price, J.L., 1994. Central olfactory connections in the macaque monkey. J. Comp. Neurol. 346, 403–434. https://doi.org/10.1002/cne.903460306.

Cecchetto, C., Fischmeister, F.P., Reichert, J.L., Bagga, D., Schöpf, V., 2019. When to collect resting-state data: the influence of odor on post-task resting-state connectivity. Neuroimage 191, 361–366. https://doi.org/10.1016/j.neuroimage.2019.02.050.

Chen, C.-F.F., Zou, D.-J., Altomare, C.G., Xu, L., Greer, C.A., Firestein, S.J., 2014. Nonsensory target-dependent organization of piriform cortex. Proc. Natl. Acad. Sci. 111, 16931–16936. https://doi.org/10.1073/pnas.1411266111.

Choi, G.B., Stettler, D.D., Kallman, B.R., Bhaskar, S.T., Fleischmann, A., Axel, R., 2011. Driving opposing behaviors with ensembles of piriform neurons. Cell 146, 1004–1015. https://doi.org/10.1016/j.cell.2011.07.041.

Choi, K., Bagen, L., Robinson, L., Umbach, G., Rugg, M., Lega, B., 2020. Longitudinal differences in human hippocampal connectivity during episodic memory processing. Cereb. Cortex Commun. 1, tgaa010 https://doi.org/10.1093/texcom/tgaa010.

Chu, S., Downes, J.J., 2000. Odour-evoked autobiographical memories: psychological investigations of proustian phenomena. Chem. Senses 25, 111–116. https://doi.org/10.1093/chemse/25.1.111.

Colombo, M., Fernandez, T., Nakamura, K., Gross, C.G., 1998. Functional differentiation along the anterior-posterior axis of the hippocampus in monkeys. J. Neurophysiol. 80, 1002–1005. https://doi.org/10.1152/jn.1998.80.2.1002.

Conti, M.Z., Vicini-Chilovi, B., Riva, M., Zanetti, M., Liberini, P., Padovani, A., Rozzini, L., 2013. Odor identification deficit predicts clinical conversion from mild cognitive impairment to dementia due to Alzheimer's disease. Arch. Clin. Neuropsychol. 28, 391–399. https://doi.org/10.1093/arclin/act032.

Cornell Karnekull, S., Jonsson, F.U., Willander, J., Sikstrom, S., Larsson, M., 2015. Long-term memory for odors: influences of familiarity and identification across 64 days. Chem. Senses 40, 259–267. https://doi.org/10.1093/chemse/bjv003.

Cornell Kärnekull, S., Arshamian, A., Willander, J., Jönsson, F.U., Nilsson, M.E., Larsson, M., 2020. The reminiscence bump is blind to blindness: evidence from sound- and odor-evoked autobiographical memory. Conscious. Cogn. 78, 102876 https://doi.org/10.1016/j.concog.2019.102876.

Courtiol, E., Wilson, D.A., 2015. The olfactory thalamus: unanswered questions about the role of the mediodorsal thalamic nucleus in olfaction. Front. Neural Circuits 9, 49. https://doi.org/10.3389/fncir.2015.00049.

Desikan, R.S., Ségonne, F., Fischl, B., Quinn, B.T., Dickerson, B.C., Blacker, D., Buckner, R.L., Dale, A.M., Maguire, R.P., Hyman, B.T., Albert, M.S., Killiany, R.J., 2006. An automated labeling system for subdividing the human cerebral cortex on MRI scans into gyral based regions of interest. Neuroimage 31, 968–980. https://doi.org/10.1016/j.neuroimage.2006.01.021.

Devanand, D.P., Lee, S., Luchsinger, J.A., Andrews, H., Goldberg, T., Huey, E.D., Schupf, N., Manly, J., Stern, Y., Kreisl, W.C., Mayeux, R., 2020. Intact global cognitive and olfactory ability predicts lack of transition to dementia. Alzheimer's Dement. 16, 326–334. https://doi.org/10.1016/j.jalz.2019.08.200.

Doty, R.L., Hawkes, C.H., 2019. Chemosensory dysfunction in neurodegenerative diseases. Handbook of Clinical Neurology. Elsevier B.V., pp. 325–360. https://doi.org/10.1016/B978-0-444-63855-7.00020-4

Eichenbaum, H., 2000. A cortical–hippocampal system for declarative memory. Nat. Rev. Neurosci. 1, 41–50. https://doi.org/10.1038/35036213.

Eichenbaum, H., Robitsek, R.J., 2009. Olfactory memory: a bridge between humans and animals in models of cognitive aging. Ann. N. Y. Acad. Sci. 1170, 658–663. https://doi.org/10.1111/j.1749-6632.2009.04012.x.

Eichenbaum, H., Otto, T., Cohen, N.J., 1994. Two functional components of the hippocampal memory system. Behav. Brain Sci. 17, 449–472. https://doi.org/10.1017/S0140525X00035391.

Ennis, M., Puche, A.C., Holy, T., Shipley, M.T., 2015. The olfactory system. The Rat Nervous System, fourth edition. Elsevier Inc., pp. 761–803. https://doi.org/10.1016/B978-0-12-374245-2.00027-9

Epstein, R.A., 2008. Parahippocampal and retrosplenial contributions to human spatial navigation. Trends Cogn. Sci. 12, 388–396. https://doi.org/10.1016/j.tics.2008.07.004.

Fanselow, M.S., Dong, H.-W., 2010. Are the dorsal and ventral hippocampus functionally distinct structures? Neuron 65, 7–19. https://doi.org/10.1016/j.neuron.2009.11.031.

Feher, J., 2017. The chemical senses. Quantitative Human Physiology. Elsevier, pp. 427–439. https://doi.org/10.1016/B978-0-12-800883-6.00039-2.

Fjaeldstad, A., Fernandes, H.M., Van Hartevelt, T.J., Gleesborg, C., Møller, A., Ovesen, T., Kringelbach, M.L., 2017. Brain fingerprints of olfaction: a novel structural method for assessing olfactory cortical networks in health and disease. Sci. Rep. 7, 42534. https://doi.org/10.1038/srep42534.

Fontanini, A., Bower, J.M., 2005. Variable coupling between olfactory system activity and respiration in Ketamine/Xylazine anesthetized rats. J. Neurophysiol. 93, 3573–3581. https://doi.org/10.1152/jn.01320.2004.

Fontanini, A., Bower, J.M., 2006. Slow-waves in the olfactory system: an olfactory perspective on cortical rhythms. Trends Neurosci. 29, 429–437. https://doi.org/10.1016/j.tins.2006.06.013.

Fontanini, A., Spano, P., Bower, J.M., 2003. Ketamine-Xylazine-induced slow (< 1.5 Hz) oscillations in the rat piriform (olfactory) cortex are functionally correlated with respiration. J. Neurosci. 23, 7993–8001. https://doi.org/10.1523/JNEUROSCI.23-22-07993.2003.

Fox, M.D., Snyder, A.Z., Vincent, J.L., Corbetta, M., Van Essen, D.C., Raichle, M.E., 2005. From the cover: the human brain is intrinsically organized into dynamic, anticorrelated functional networks. Proc. Natl. Acad. Sci. 102, 9673–9678. https://doi.org/10.1073/pnas.0504136102.

Fox, K.C.R., Foster, B.L., Kucyi, A., Daitch, A.L., Parvizi, J., 2018. Intracranial electrophysiology of the human default network. Trends Cogn. Sci. 22, 307–324. https://doi.org/10.1016/J.TICS.2018.02.002.

Galambos, R., Sheatz, G., Vernier, V.G., 1956. Electrophysiological correlates of a conditioned response in cats. Science (80-.) 123, 376–377. https://doi.org/10.1126/science.123.3192.376.

Gass, N., Schwarz, A.J., Sartorius, A., Schenker, E., Risterucci, C., Spedding, M., Zheng, L., Meyer-Lindenberg, A., Weber-Fahr, W., 2014. Sub-anesthetic ketamine modulates intrinsic BOLD connectivity within the hippocampal-prefrontal circuit in the rat. Neuropsychopharmacology 39, 895–906. https://doi.org/10.1038/npp.2013.290.

Gewirtz, J.C., McNish, K.A., Davis, M., 2000. Is the hippocampus necessary for contextual fear conditioning? Behav. Brain Res. 110, 83–95. https://doi.org/10.1016/S0166-4328(99)00187-4.

Gire, D.H., Restrepo, D., Sejnowski, T.J., Greer, C., De Carlos, J.A., Lopez-Mascaraque, L., 2013. Temporal processing in the olfactory system: can we see a smell? Neuron 78, 416–432. https://doi.org/10.1016/j.neuron.2013.04.033.

Gonçalves Pereira, P.M., Insausti, R., Artacho-Pérula, E., Salmenperä, T., Kälviäinen, R., Pitkänen, A., 2005. MR volumetric analysis of the piriform cortex and cortical amygdala in drug-refractory temporal lobe epilepsy. AJNR Am. J. Neuroradiol. 26, 319–332.

Gottfried, J.A., 2010. Central mechanisms of odour object perception. Nat. Rev. Neurosci. 11, 628–641. https://doi.org/10.1038/nrn2883.

Gottfried, J.A., Dolan, R.J., 2003. The nose smells what the eye sees: crossmodal visual facilitation of human olfactory perception. Neuron 39, 375–386. https://doi.org/10.1016/S0896-6273(03)00392-1.

Gottfried, J.A., Deichmann, R., Winston, J.S., Dolan, R.J., 2002. Functional heterogeneity in human olfactory cortex: an event-related functional magnetic resonance imaging study. J. Neurosci. 22, 10819–10828. https://doi.org/10.1523/jneurosci.22-24-10819.2002.

Gottfried, J.A., Smith, A.P., Rugg, M.D., Dolan, R.J., 2004. Remembrance of odors past: human olfactory cortex in cross-modal recognition memory. Neuron 42, 687–695. https://doi.org/10.1016/S0896-6273(04)00270-3.

Gottfried, J.A., Winston, J.S., Dolan, R.J., 2006. Dissociable codes of odor quality and odorant structure in human piriform cortex. Neuron 49, 467–479. https://doi.org/10.1016/j.neuron.2006.01.007.

Goulas, A., Margulies, D.S., Bezgin, G., Hilgetag, C.C., 2019. The architecture of mammalian cortical connectomes in light of the theory of the dual origin of the cerebral cortex. Cortex 118, 244–261. https://doi.org/10.1016/j.cortex.2019.03.002.

Greicius, M.D., Krasnow, B., Reiss, A.L., Menon, V., 2003. Functional connectivity in the resting brain: a network analysis of the default mode hypothesis. Proc. Natl. Acad. Sci. U. S. A. 100, 253–258. https://doi.org/10.1073/pnas.0135058100.

Haberly, L.B., 2001. Parallel-distributed processing in olfactory cortex: new insights from morphological and physiological analysis of neuronal circuitry. Chem. Senses 26, 551–576. https://doi.org/10.1093/chemse/26.5.551.

Hasselmo, M.E., McClelland, J.L., 1999. Neural models of memory. Curr. Opin. Neurobiol. 9, 184–188. https://doi.org/10.1016/S0959-4388(99)80025-7.

Heck, D.H., McAfee, S.S., Liu, Y., Babajani-Feremi, A., Rezaie, R., Freeman, W.J., Wheless, J.W., Papanicolaou, A.C., Ruszinko, M., Kozma, R., 2016. Cortical rhythms are modulated by respiration, bioRxiv. Cold Spring Harbor Labs Journals. https://doi.org/10.1101/049007.

Heck, D.H., McAfee, S.S., Liu, Y., Babajani-Feremi, A., Rezaie, R., Freeman, W.J., Wheless, J.W., Papanicolaou, A.C., Ruszinkó, M., Sokolov, Y., Kozma, R., 2017. Breathing as a fundamental rhythm of brain function. Front. Neural Circuits 10, 115. https://doi.org/10.3389/fncir.2016.00115.

Heck, D.H., Kozma, R., Kay, L.M., 2019. The rhythm of memory: how breathing shapes memory function. J. Neurophysiol. 122, 563–571. https://doi.org/10.1152/jn.00200.2019.

Héctor, R.-F., Eduardo, B.-P., Pilar, D.-S., Diana, P.-N., Julio, G., Silvia, H.-T., 2019. Characterization of the olfactory pathway by anisotropic diffusion using nuclear magnetic resonance imaging in a pediatric population. Int. J. Radiol. Imaging Tech. 5, 057. https://doi.org/10.23937/2572-3235.1510057.

Henderson, J.M., Larson, C.L., Zhu, D.C., 2008. Full scenes produce more activation than close-up scenes and scene-diagnostic objects in parahippocampal and retrosplenial cortex: an fMRI study. Brain Cogn. 66, 40–49. https://doi.org/10.1016/j.bandc.2007.05.001.

Herrero, J.L., Khuvis, S., Yeagle, E., Cerf, M., Mehta, A.D., 2018. Breathing above the brain stem: volitional control and attentional modulation in humans. J. Neurophysiol. 119, 145–159. https://doi.org/10.1152/jn.00551.2017.

Herrick, C.J., 1933. The functions of the olfactory parts of the cerebral cortex. Proc. Natl. Acad. Sci. 19, 7–14. https://doi.org/10.1073/pnas.19.1.7.

Herz, R.S., Engen, T., 1996. Odor memory: review and analysis. Psychon. Bull. Rev. 3, 300–313. https://doi.org/10.3758/BF03210754.

Herz, R.S., von Clef, J., 2001. The influence of verbal labeling on the perception of odors: evidence for olfactory illusions? Perception 30, 381–391. https://doi.org/10.1068/p3179.

Herz, R.S., Eliassen, J., Beland, S., Souza, T., 2004. Neuroimaging evidence for the emotional potency of odor-evoked memory. Neuropsychologia 42, 371–378. https://doi.org/10.1016/j.neuropsychologia.2003.08.009.

Hinds, O.P., Rajendran, N., Polimeni, J.R., Augustinack, J.C., Wiggins, G., Wald, L.L., Diana Rosas, H., Potthast, A., Schwartz, E.L., Fischl, B., 2008. Accurate prediction of V1 location from cortical folds in a surface coordinate system. Neuroimage 39, 1585–1599. https://doi.org/10.1016/j.neuroimage.2007.10.033.

Ho, J.W., Burwell, R.D., 2014. Perirhinal and postrhinal functional inputs to the hippocampus. Space, Time and Memory in the Hippocampal Formation. Springer-Verlag, Wien, pp. 55–81. https://doi.org/10.1007/978-3-7091-1292-2_3.

Howard, J.D., Plailly, J., Grueschow, M., Haynes, J.-D., Gottfried, J.A., 2009. Odor quality coding and categorization in human posterior piriform cortex. Nat. Neurosci. 12, 932–938. https://doi.org/10.1038/nn.2324.

Howell, A.L., Osher, D.E., Li, J., Saygin, Z.M., 2020. The intrinsic neonatal hippocampal network: rsfMRI findings. J. Neurophysiol. 124, 1458–1468. https://doi.org/10.1152/jn.00362.2020.

Hummel, T., Reden, K.R.J., Hähner, A., Weidenbecher, M., Hüttenbrink, K.B., 2009. Effects of olfactory training in patients with olfactory loss. Laryngoscope 119, 496–499. https://doi.org/10.1002/lary.20101.

Illig, K.R., Wilson, D.A., 2009. Olfactory cortex: comparative anatomy. In: Kaas, J. (Ed.), Encyclopedia of Neuroscience. Elsevier, New York, NY, pp. 101–106. https://doi.org/10.1016/B978-008045046-9.00971-2.

Janzen, G., Van Turennout, M., 2004. Selective neural representation of objects rellevant for navigation. Nat. Neurosci. 7, 673–677. https://doi.org/10.1038/nn1257.

Jenkinson, M., Beckmann, C.F., Behrens, T.E.J., Woolrich, M.W., Smith, S.M., 2012. FSL. Neuroimage 62, 782–790. https://doi.org/10.1016/j.neuroimage.2011.09.015.

Johnson, D.M., Illig, K.R., Behan, M., Haberly, L.B., 2000. New features of connectivity in piriform cortex visualized by intracellular injection of pyramidal cells suggest that "primary" olfactory cortex functions like "association" cortex in other sensory systems. J. Neurosci. 20, 6974–6982. https://doi.org/10.1523/jneurosci.20-18-06974.2000.

Kadohisa, M., Wilson, D.A., 2006. Separate encoding of identity and similarity of complex familiar odors in piriform cortex. Proc. Natl. Acad. Sci. U. S. A. 103, 15206–15211. https://doi.org/10.1073/pnas.0604313103.

Kahn, I., Andrews-Hanna, J.R., Vincent, J.L., Snyder, A.Z., Buckner, R.L., 2008. Distinct cortical anatomy linked to subregions of the medial temporal lobe revealed by intrinsic functional connectivity. J. Neurophysiol. 100, 129–139. https://doi.org/10.1152/jn.00077.2008.

Kareken, D.A., Sabri, M., Radnovich, A.J., Claus, E., Foresman, B., Hector, D., Hutchins, G.D., 2004. Olfactory system activation from sniffing: effects in piriform and orbitofrontal cortex. Neuroimage 22, 456–465. https://doi.org/10.1016/j.neuroimage.2004.01.008.

Karunanayaka, P., Eslinger, P.J., Wang, J.-L., Weitekamp, C.W., Molitoris, S., Gates, K. M., Molenaar, P.C.M., Yang, Q.X., 2014. Networks involved in olfaction and their dynamics using independent component analysis and unified structural equation modeling. Hum. Brain Mapp. 35, 2055–2072. https://doi.org/10.1002/hbm.22312.

Karunanayaka, P.R., Wilson, D.A., Vasavada, M., Wang, J., Martinez, B., Tobia, M.J., Kong, L., Eslinger, P., Yang, Q.X., 2015. Rapidly acquired multisensory association in the olfactory cortex. Brain Behav. 5, e00390 https://doi.org/10.1002/brb3.390.

Karunanayaka, P., Tobia, M.J., Yang, Q.X., 2017. Age-related resting-state functional connectivity in the olfactory and trigeminal networks. Neuroreport 28, 943–948. https://doi.org/10.1097/wnr.0000000000000850.

Kay, L.M., 2005. Theta oscillations and sensorimotor performance. Proc. Natl. Acad. Sci. U. S. A. 102, 3863–3868. https://doi.org/10.1073/pnas.0407920102.

Kay, L.M., 2014. Circuit oscillations in odor perception and memory. Prog. Brain Res. 208, 223–251. https://doi.org/10.1016/B978-0-444-63350-7.00009-7.

Kay, L.M., Stopfer, M., 2006. Information processing in the olfactory systems of insects and vertebrates. Semin. Cell Dev. Biol. 17, 433–442. https://doi.org/10.1016/j.semcdb.2006.04.012.

Kay, L.M., Beshel, J., Brea, J., Martin, C., Rojas-Líbano, D., Kopell, N., 2009. Olfactory oscillations: the what, how and what for. Trends Neurosci. 32, 207–214. https://doi.org/10.1016/j.tins.2008.11.008.

Kepecs, A., Uchida, N., Mainen, Z.F., 2006. The sniff as a unit of olfactory processing. Chem. Senses 31, 167–179. https://doi.org/10.1093/chemse/bjj016.

Kiparizoska, S., Ikuta, T., 2017. Disrupted olfactory integration in schizophrenia: functional connectivity study. Int. J. Neuropsychopharmacol. 20, 740–746. https://doi.org/10.1093/ijnp/pyx045.

Kollndorfer, K., Fischmeister, F.P.S., Kowalczyk, K., Hoche, E., Mueller, C.A., Trattnig, S., Schöpf, V., 2015. Olfactory training induces changes in regional functional connectivity in patients with long-term smell loss. Neuroimage Clin. 9, 401–410. https://doi.org/10.1016/j.nicl.2015.09.004.

Komiyama, T., Luo, L., 2006. Development of wiring specificity in the olfactory system. Curr. Opin. Neurobiol. 16, 67–73. https://doi.org/10.1016/j.conb.2005.12.002.

Koritnik, B., Azam, S., Andrew, C.M., Leigh, P.N., Williams, S.C.R., 2009. Imaging the brain during sniffing: a pilot fMRI study. Pulm. Pharmacol. Ther. 22, 97–101. https://doi.org/10.1016/j.pupt.2008.10.009.

Krusemark, E.A., Li, W., 2012. Enhanced olfactory sensory perception of threat in anxiety: an event-related fMRI study. Chemosens. Percept. 5, 37–45. https://doi.org/10.1007/s12078-011-9111-7.

Kucyi, A., Schrouff, J., Bickel, S., Foster, B.L., Shine, J.M., Parvizi, J., 2018. Intracranial electrophysiology reveals reproducible intrinsic functional connectivity within human brain networks. J. Neurosci. 38, 4230–4242. https://doi.org/10.1523/JNEUROSCI.0217-18.2018.

Lakatos, P., Chen, C.-M., O'Connell, M.N., Mills, A., Schroeder, C.E., 2007. Neuronal oscillations and multisensory interaction in primary auditory cortex. Neuron 53, 279–292. https://doi.org/10.1016/j.neuron.2006.12.011.

Lane, G., Zhou, G., Noto, T., Zelano, C., 2020. Assessment of direct knowledge of the human olfactory system. Exp. Neurol. 329, 113304 https://doi.org/10.1016/j.expneurol.2020.113304.

Lawless, H.T., 1978. Recognition of common odors, pictures, and simple shapes. Percept. Psychophys. 24, 493–495. https://doi.org/10.3758/BF03198772.

Lee, T.S., Mumford, D., Romero, R., Lamme, V.A.F., 1998. The role of the primary visual cortex in higher level vision. Vision Res. 38, 2429–2454. https://doi.org/10.1016/S0042-6989(97)00464-1.

Lee, T.S., Yang, C.F., Romero, R.D., Mumford, D., 2002. Neural activity in early visual cortex reflects behavioral experience and higher-order perceptual saliency. Nat. Neurosci. 5, 589–597. https://doi.org/10.1038/nn0602-860.

Levinson, M., Kolenda, J.P., Alexandrou, G.J., Escanilla, O., Cleland, T.A., Smith, D.M., Linster, C., 2020. Context-dependent odor learning requires the anterior olfactory nucleus. Behav. Neurosci. 134, 332–343. https://doi.org/10.1037/bne0000371.

Li, W., Luxenberg, E., Parrish, T., Gottfried, J.A., 2006. Learning to smell the roses: experience-dependent neural plasticity in human piriform and orbitofrontal cortices. Neuron 52, 1097–1108. https://doi.org/10.1016/j.neuron.2006.10.026.

Li, W., Howard, J.D., Parrish, T.B., Gottfried, J.A., 2008. Aversive learning enhances perceptual and cortical discrimination of indiscriminable odor cues. Science 319, 1842–1845. https://doi.org/10.1126/science.1152837.

Libby, L.A., Ekstrom, A.D., Daniel Ragland, J., Ranganath, C., 2012. Differential connectivity of perirhinal and parahippocampal cortices within human hippocampal subregions revealed by high-resolution functional imaging. J. Neurosci. 32, 6550–6560. https://doi.org/10.1523/JNEUROSCI.3711-11.2012.

Liska, A., Galbusera, A., Schwarz, A.J., Gozzi, A., 2015. Functional connectivity hubs of the mouse brain. Neuroimage 115, 281–291. https://doi.org/10.1016/j.neuroimage.2015.04.033.

Liu, Y., McAfee, S.S., Heck, D.H., 2017. Hippocampal sharp-wave ripples in awake mice are entrained by respiration. Sci. Rep. 7, 8950. https://doi.org/10.1038/s41598-017-09511-8.

Lockmann, A.L.V., Tort, A.B.L., 2018. Nasal respiration entrains delta-frequency oscillations in the prefrontal cortex and hippocampus of rodents. Brain Struct. Funct. 223, 1–3. https://doi.org/10.1007/s00429-017-1573-1.

Lockmann, A.L.V., Laplagne, D.A., Leão, R.N., Tort, A.B.L., 2016. A respiration-coupled rhythm in the rat hippocampus independent of theta and slow oscillations. J. Neurosci. 36, 5338–5352. https://doi.org/10.1523/JNEUROSCI.3452-15.2016.

Lockmann, A.L.V., Laplagne, D.A., Tort, A.B.L., 2018. Olfactory bulb drives respiration-coupled beta oscillations in the rat hippocampus. Eur. J. Neurosci. 48, 2663–2673. https://doi.org/10.1111/ejn.13665.

Logothetis, N.K., Eschenko, O., Murayama, Y., Augath, M., Steudel, T., Evrard, H.C., Besserve, M., Oeltermann, A., 2012. Hippocampal-cortical interaction during periods of subcortical silence. Nature 491, 547–553. https://doi.org/10.1038/nature11618.

Lu, H., Zou, Q., Gu, H., Raichle, M.E., Stein, E.A., Yang, Y., 2012. Rat brains also have a default mode network. Proc. Natl. Acad. Sci. U. S. A. 109, 3979–3984. https://doi.org/10.1073/pnas.1200506109.

Lu, Testa, Jordan, Elyan, Kanekar, Wang, Eslinger, Yang, Zhang, Karunanayaka, 2019. Functional connectivity between the resting-state olfactory network and the hippocampus in Alzheimer's disease. Brain Sci. 9, 338. https://doi.org/10.3390/brainsci9120338.

Luna, R., Hernández, A., Brody, C.D., Romo, R., 2005. Neural codes for perceptual discrimination in primary somatosensory cortex. Nat. Neurosci. 8, 1210–1219. https://doi.org/10.1038/nn1513.

Macrides, F., 1975. Temporal relationships between hippocampal slow waves and exploratory sniffing in hamsters. Behav. Biol. 14, 295–308. https://doi.org/10.1016/S0091-6773(75)90419-8.

Macrides, F., Eichenbaum, H., Forbes, W., 1982. Temporal relationship between sniffing and the limbic theta rhythm during odor discrimination reversal learning. J. Neurosci. 2, 1705–1717. https://doi.org/10.1523/JNEUROSCI.02-12-01705.1982.

Madore, K.P., Szpunar, K.K., Addis, D.R., Schacter, D.L., 2016. Episodic specificity induction impacts activity in a core brain network during construction of imagined future experiences. Proc. Natl. Acad. Sci. U. S. A. 113, 10696–10701. https://doi.org/10.1073/pnas.1612278113.

Mai, J.K., Paxinos, G., 2012. The Human Nervous System, 3rd ed. Elsevier. https://doi.org/10.1016/c2009-0-02721-4.

Mai, J.K., Majtanik, M., Paxinos, G., 2015. Atlas of the Human Brain, 4th ed. Academic Press.

Mainland, J., Sobel, N., 2006. The sniff is part of the olfactory percept. Chem. Senses 31, 181–196. https://doi.org/10.1093/chemse/bjj012.

Mainland, J.D., Lundström, J.N., Reisert, J., Lowe, G., 2014. From molecule to mind: an integrative perspective on odor intensity. Trends Neurosci. 37, 443–454. https://doi.org/10.1016/j.tins.2014.05.005.

Margulies, D.S., Ghosh, S.S., Goulas, A., Falkiewicz, M., Huntenburg, J.M., Langs, G., Bezgin, G., Eickhoff, S.B., Castellanos, F.X., Petrides, M., Jefferies, E., Smallwood, J., 2016. Situating the default-mode network along a principal gradient of macroscale cortical organization. Proc. Natl. Acad. Sci. 113, 12574–12579. https://doi.org/10.1073/pnas.1608282113.

Martin, C., Ravel, N., 2014. Beta and gamma oscillatory activities associated with olfactory memory tasks: different rhythms for different functional networks? Front. Behav. Neurosci. 23, 218. https://doi.org/10.3389/fnbeh.2014.00218.

Martin, C., Gervais, R., Messaoudi, B., Ravel, N., 2006. Learning-induced oscillatory activities correlated to odour recognition: a network activity. Eur. J. Neurosci. 23, 1801–1810. https://doi.org/10.1111/j.1460-9568.2006.04711.x.

Martin, C., Beshel, J., Kay, L.M., 2007. An olfacto-hippocampal network is dynamically involved in odor-discrimination learning. J. Neurophysiol. 98, 2196–2205. https://doi.org/10.1152/jn.00524.2007.

Masaoka, Y., Koiwa, N., Homma, I., 2005. Inspiratory phase-locked alpha oscillation in human olfaction: source generators estimated by a dipole tracing method. J. Physiol. 566, 979–997. https://doi.org/10.1113/jphysiol.2005.086124.

McGann, J.P., 2017. Poor human olfaction is a 19th-century myth. Science 356, eaam7263. https://doi.org/10.1126/science.aam7263.

McNamara, A.M., Magidson, P.D., Linster, C., Wilson, D.A., Cleland, T.A., 2008. Distinct neural mechanisms mediate olfactory memory formation at different timescales. Learn. Mem. 15, 117–125. https://doi.org/10.1101/lm.785608.

McNish, K.A., Gewirtz, J.C., Davis, M., 2000. Disruption of contextual freezing, but not contextual blocking of fear-potentiated startle, after lesions of the dorsal hippocampus. Behav. Neurosci. 114, 64–76. https://doi.org/10.1037/0735-7044.114.1.64.

Mechling, A.E., Hübner, N.S., Lee, H.-L., Hennig, J., von Elverfeldt, D., Harsan, L.-A., 2014. Fine-grained mapping of mouse brain functional connectivity with resting-

state fMRI. Neuroimage 96, 203–215. https://doi.org/10.1016/j.neuroimage.2014.03.078.
Meredith, M.A., Allman, B.L., 2015. Single-unit analysis of somatosensory processing in the core auditory cortex of hearing ferrets. Eur. J. Neurosci. 41, 686–698. https://doi.org/10.1111/ejn.12828.
Mesulam, M.-M., 1998. From sensation to cognition. Brain 121, 1013–1052. https://doi.org/10.1093/brain/121.6.1013.
Meunier, D., Fonlupt, P., Saive, A.L., Plailly, J., Ravel, N., Royet, J.P., 2014. Modular structure of functional networks in olfactory memory. Neuroimage 95, 264–275. https://doi.org/10.1016/j.neuroimage.2014.03.041.
Milardi, D., Cacciola, A., Calamuneri, A., Ghilardi, M.F., Caminiti, F., Cascio, F., Andronaco, V., Anastasi, G., Mormina, E., Arrigo, A., Bruschetta, D., Quartarone, A., 2017. The olfactory system revealed: non-invasive mapping by using constrained spherical deconvolution tractography in healthy humans. Front. Neuroanat. 11, 32. https://doi.org/10.3389/fnana.2017.00032.
Miles, A.N., Berntsen, D., 2011. Odour-induced mental time travel into the past and future: do odour cues retain a unique link to our distant past? Memory 19, 930–940. https://doi.org/10.1080/09658211.2011.613847.
Moser, M.B., Moser, E.I., 1998. Functional differentiation in the hippocampus. Hippocampus 8, 608–619. https://doi.org/10.1002/(SICI)1098-1063(1998)8:6<608::AID-HIPO3>3.0.CO;2-7.
Moss, A., Miles, C., Elsley, J., Johnson, A.J., 2019. Olfactory working memory: exploring the differences in n-back memory for high and low verbalisable odorants. Memory 27, 1319–1344. https://doi.org/10.1080/09658211.2019.1653469.
Murphy, C., 2019. Olfactory and other sensory impairments in Alzheimer disease. Nat. Rev. Neurol. 15, 11–24. https://doi.org/10.1038/s41582-018-0097-5.
Murray, E.A., Richmond, B.J., 2001. Role of perirhinal cortex in object perception, memory, and associations. Curr. Opin. Neurobiol. 11, 188–193. https://doi.org/10.1016/S0959-4388(00)00195-1.
Nguyen Chi, V., Müller, C., Wolfenstetter, T., Yanovsky, Y., Draguhn, A., Tort, A.B.L., Brankačk, J., 2016. Hippocampal respiration-driven rhythm distinct from theta oscillations in awake mice. J. Neurosci. 36, 162–177. https://doi.org/10.1523/JNEUROSCI.2848-15.2016.
Nigri, A., Ferraro, S., D'Incerti, L., Critchley, H.D., Bruzzone, M.G., Minati, L., D'Incerti, L., Critchley, H.D., Bruzzone, M.G., Minati, L., 2013. Connectivity of the amygdala, piriform, and orbitofrontal cortex during olfactory stimulation: a functional MRI study. Neuroreport 24, 171–175. https://doi.org/10.1097/wnr.0b013e32835d5d2b.
Norman, G., Eacott, M.J., 2005. Dissociable effects of lesions to the perirhinal cortex and the postrhinal cortex on memory for context and objects in rats. Behav. Neurosci. 119, 557–566. https://doi.org/10.1037/0735-7044.119.2.557.
Noto, T., Zhou, G., Schuele, S., Templer, J., Zelano, C., 2018. Automated analysis of breathing waveforms using BreathMetrics: a respiratory signal processing toolbox. Chem. Senses 43, 583–597. https://doi.org/10.1093/chemse/bjy045.
Olofsson, J.K., Gottfried, J.A., 2015. The muted sense: neurocognitive limitations of olfactory language. Trends Cogn. Sci. (Regul. Ed.) 19, 314–321. https://doi.org/10.1016/j.tics..2015.04.007.
Olofsson, J.K., Rogalski, E., Harrison, T., Mesulam, M.-M., Gottfried, J.A., 2013. A cortical pathway to olfactory naming: evidence from primary progressive aphasia. Brain 136, 1245–1259. https://doi.org/10.1093/brain/awt019.
Olofsson, J.K., Zhou, G., East, B.S., Zelano, C., Wilson, D.A., 2019. Odor identification in rats: behavioral and electrophysiological evidence of learned olfactory-auditory associations. eneuro 6. ENEURO. https://doi.org/10.1523/ENEURO.0102-19.2019, 0102-19.2019.
Oostenveld, R., Fries, P., Maris, E., Schoffelen, J.-M., 2011. FieldTrip: open source software for advanced analysis of MEG, EEG, and invasive electrophysiological data. Comput. Intell. Neurosci. 2011, 156869 https://doi.org/10.1155/2011/156869.
Otto, T., Eichenbaum, H., Wible, C.G., Wiener, S.I., 1991a. Learning-related patterns of CA1 spike trains parallel stimulation parameters optimal for inducing hippocampal long-term potentiation. Hippocampus 1, 181–192. https://doi.org/10.1002/hipo.450010206.
Otto, T., Schottler, F., Staubli, U., Eichenbaum, H., Lynch, G., 1991b. Hippocampus and olfactory discrimination learning: effects of entorhinal cortex lesions on olfactory learning and memory in a successive-cue, go–no-go task. Behav. Neurosci. 105, 111–119. https://doi.org/10.1037/0735-7044.105.1.111.
Pashkovski, S.L., Iurilli, G., Brann, D., Chicharro, D., Drummey, K., Franks, K., Panzeri, S., Datta, S.R., 2020. Structure and flexibility in cortical representations of odour space. Nature 583, 253–258. https://doi.org/10.1038/s41586-020-2451-1.
Peter, M.G., Fransson, P., Mårtensson, G., Postma, E.M., Nordin, L.E., Westman, E., Boesveldt, S., Lundström, J.N., 2021. Normal olfactory functional connectivity despite lifelong absence of olfactory experiences. Cereb. Cortex 31, 159–168. https://doi.org/10.1093/cercor/bhaa217.
Plailly, J., Villalba, M., Vallat, R., Nicolas, A., Ruby, P., 2019. Incorporation of fragmented visuo-olfactory episodic memory into dreams and its association with memory performance. Sci. Rep. 9, 1–14. https://doi.org/10.1038/s41598-019-51497-y.
Poppenk, J., Evensmoen, H.R., Moscovitch, M., Nadel, L., 2013. Long-axis specialization of the human hippocampus. Trends Cogn. Sci. 17, 230–240. https://doi.org/10.1016/j.tics.2013.03.005.
Porada, D.K., Regenbogen, C., Seubert, J., Freiherr, J., Lundström, J.N., 2019. Multisensory enhancement of odor object processing in primary olfactory cortex. Neuroscience 418, 254–265. https://doi.org/10.1016/j.neuroscience.2019.08.040.
Price, J.L., 1990. Olfactory system. In: Paxinos, G. (Ed.), The Human Nervous System. Academic Press, San Diego, pp. 979–1001.
Price, J.L., 2009. Olfactory Higher centers anatomy. Encyclopedia of Neuroscience. Elsevier, pp. 129–136. https://doi.org/10.1016/B978-008045046-9.01692-2.
Proust, M., 1922. Swann's Way, Remembrance of Things Past, Volume One [WWW Document]. URL https://www.gutenberg.org/files/7178/7178-h/7178-h.htm (accessed 6.7.20).
Ranganath, C., Ritchey, M., 2012. Two cortical systems for memory-guided behaviour. Nat. Rev. Neurosci. 13, 713–726. https://doi.org/10.1038/nrn3338.
Rauschecker, J.P., 1999. Auditory cortical plasticity: a comparison with other sensory systems. Trends Neurosci. 22, 74–80. https://doi.org/10.1016/S0166-2236(98)01303-4.
Rebello, M.R., McTavish, T.S., Willhite, D.C., Short, S.M., Shepherd, G.M., Verhagen, J.V., 2014. Perception of odors linked to precise timing in the olfactory system. PLoS Biol. 12, e1002021 https://doi.org/10.1371/journal.pbio.1002021.
Roesch, M.R., Stalnaker, T.A., Schoenbaum, G., 2006. Associative encoding in anterior piriform cortex versus orbitofrontal cortex during odor discrimination and reversal learning. Cereb. Cortex 17, 643–652. https://doi.org/10.1093/cercor/bhk009.
Rojas-Líbano, D., Frederick, D.E., Egaña, J., Kay, L.M., 2014. The olfactory bulb theta rhythm follows all frequencies of diaphragmatic respiration in the freely behaving rat. Front. Behav. Neurosci. 8, 214. https://doi.org/10.3389/fnbeh.2014.00214.
Roland, B., Deneux, T., Franks, K.M., Bathellier, B., Fleischmann, A., 2017. Odor identity coding by distributed ensembles of neurons in the mouse olfactory cortex. Elife 6, e26337. https://doi.org/10.7554/eLife.26337.
Sacco, T., Sacchetti, B., 2010. Role of secondary sensory cortices in emotional memory storage and retrieval in rats. Science 329, 649–656. https://doi.org/10.1126/science.1183165.
Saive, A.-L.L., Royet, J.-P.P., Plailly, J., 2014. A review on the neural bases of episodic odor memory: from laboratory-based to autobiographical approaches. Front. Behav. Neurosci. 8, 240. https://doi.org/10.3389/fnbeh.2014.00240.
Saive, A.-L., Royet, J.-P., Garcia, S., Thévenet, M., Plailly, J., 2015. "What-where-which" episodic retrieval requires conscious recollection and is promoted by semantic knowledge. PLoS One 10, e0143767. https://doi.org/10.1371/journal.pone.0143767.
Schoenbaum, G., Eichenbaum, H., 1995. Information coding in the rodent prefrontal cortex. I. Single-neuron activity in orbitofrontal cortex compared with that in pyriform cortex. J. Neurophysiol. 74, 733–750. https://doi.org/10.1152/jn.1995.74.2.733.
Schroeder, C., Molhom, S., Lakatos, P., Ritter, W., Foxe, J., 2004. Human-simian correspondence in the early cortical processing of multisensory cues. Cogn. Process. 5, 140–151. https://doi.org/10.1007/s10339-004-0020-4.
Schwarz, A.J., Gass, N., Sartorius, A., Zheng, L., Spedding, M., Schenker, E., Risterucci, C., Meyer-Lindenberg, A., Weber-Fahr, W., 2013. The low-frequency blood oxygenation level-dependent functional connectivity signature of the hippocampal-prefrontal network in the rat brain. Neuroscience 228, 243–258. https://doi.org/10.1016/j.neuroscience.2012.10.032.
Sepulcre, J., Sabuncu, M.R., Yeo, T.B., Liu, H., Johnson, K.A., 2012. Stepwise connectivity of the modal cortex reveals the multimodal organization of the human brain. J. Neurosci. 32, 10649–10661. https://doi.org/10.1523/JNEUROSCI.0759-12.2012.
Shusterman, R., Smear, M.C., Koulakov, A.A., Rinberg, D., 2011. Precise olfactory responses tile the sniff cycle. Nat. Neurosci. 14, 1039–1044. https://doi.org/10.1038/nn.2877.
Skopin, M.D., Bayat, A., Kurada, L., Siddu, M., Joshi, S., Zelano, C.M., Koubeissi, M.Z., 2020. Epileptogenesis-induced changes of hippocampal-piriform connectivity. Seizure 81, 1–7. https://doi.org/10.1016/j.seizure.2020.07.008.
Smear, M., Shusterman, R., O'Connor, R., Bozza, T., Rinberg, D., 2011. Perception of sniff phase in mouse olfaction. Nature 479, 397–400. https://doi.org/10.1038/nature10521.
Smith, S.M., 2002. Fast robust automated brain extraction. Hum. Brain Mapp. 17, 143–155. https://doi.org/10.1002/hbm.10062.
Smith, S.M., Jenkinson, M., Woolrich, M.W., Beckmann, C.F., Behrens, T.E.J., Johansen-Berg, H., Bannister, P.R., De Luca, M., Drobnjak, I., Flitney, D.E., Niazy, R.K., Saunders, J., Vickers, J., Zhang, Y., De Stefano, N., Brady, J.M., Matthews, P.M., 2004. Advances in functional and structural MR image analysis and implementation as FSL. Neuroimage 23 (Suppl 1), S208–S219. https://doi.org/10.1016/j.neuroimage.2004.07.051.
Sobel, N., Prabhakaran, V., Desmond, J.E., Glover, G.H., Goode, R.L., Sullivan, E.V., Gabrieli, J.D., 1998a. Sniffing and smelling: separate subsystems in the human olfactory cortex. Nature 392, 282–286. https://doi.org/10.1038/32654.
Sobel, N., Prabhakaran, V., Hartley, C.A., Desmond, J.E., Zhao, Z., Glover, G.H., Gabrieli, J.D.E., Sullivan, E.V., 1998b. Odorant-induced and sniff-induced activation in the cerebellum of the human. J. Neurosci. 18, 8990–9001. https://doi.org/10.1523/JNEUROSCI.18-21-08990.1998.
Sobel, N., Prabhakaran, V., Hartley, C.A., Desmond, J.E., Glover, G.H., Sullivan, E.V., Gabrieli, J.D., 1999. Blind smell: brain activation induced by an undetected airborne chemical. Brain 122 (Pt 2), 209–217. https://doi.org/10.1093/brain/122.2.209.
Sobel, N., Prabhakaran, V., Zhao, Z., Desmond, J.E., Glover, G.H., Sullivan, E.V., Gabrieli, J.D.E., 2000. Time course of odorant-induced activation in the human primary olfactory cortex. J. Neurophysiol. 83, 537–551. https://doi.org/10.1152/jn.2000.83.1.537.
Squire, L.R., Zola, S.M., 1996. Structure and function of declarative and nondeclarative memory systems. Proc. Natl. Acad. Sci. 93, 13515–13522. https://doi.org/10.1073/pnas.93.24.13515.
Sreenivasan, K., Zhuang, X., Banks, S.J., Mishra, V., Yang, Z., Deshpande, G., Cordes, D., 2017. Olfactory network differences in master sommeliers: connectivity analysis using Granger causality and graph theoretical approach. Brain Connect. 7, 123–136. https://doi.org/10.1089/brain.2016.0458.

Stam, C.J., Nolte, G., Daffertshofer, A., 2007. Phase lag index: assessment of functional connectivity from multi channel EEG and MEG with diminished bias from common sources. Hum. Brain Mapp. 28, 1178–1193. https://doi.org/10.1002/hbm.20346.

Stanciu, I., Larsson, M., Nordin, S., Adolfsson, R., Nilsson, L.-G., Olofsson, J.K., 2014. Olfactory impairment and subjective olfactory complaints independently predict conversion to dementia: a longitudinal, population-based study. J. Int. Neuropsychol. Soc. 20, 209–217. https://doi.org/10.1017/S1355617713001409.

Staubli, U., Fraser, D., Kessler, M., Lynch, G., 1986. Studies on retrograde and anterograde amnesia of olfactory memory after denervation of the hippocampus by entorhinal cortex lesions. Behav. Neural Biol. 46, 432–444. https://doi.org/10.1016/S0163-1047(86)90464-4.

Strange, B.A., Witter, M.P., Lein, E.S., Moser, E.I., 2014. Functional organization of the hippocampal longitudinal axis. Nat. Rev. Neurosci. 15, 655–669. https://doi.org/10.1038/nrn3785.

Striedter, G.F., Northcutt, R.G., 2020. Brains Through Time: A Natural History of Vertebrates. Oxford University Press.

Sullivan, R.M., 2003. Molecular biology of early olfactory memory. Learn. Mem. 10, 1–4. https://doi.org/10.1101/lm.58203.

Sullivan, R.M., Wilson, D.A., Ravel, N., Mouly, A.-M., 2015. Olfactory memory networks: from emotional learning to social behaviors. Front. Behav. Neurosci. 9, 36. https://doi.org/10.3389/fnbeh.2015.00036.

Sunwoo, M.K., Cha, J., Ham, J.H., Song, S.K., Hong, J.Y., Lee, J.-M., Sohn, Y.H., Lee, P. H., 2015. Olfactory performance and resting state functional connectivity in non-demented drug naïve patients with Parkinson's disease. Hum. Brain Mapp. 36, 1716–1727. https://doi.org/10.1002/hbm.22732.

Tak, S., Polimeni, J.R., Wang, D.J.J., Yan, L., Chen, J.J., 2015. Associations of resting-state fMRI functional connectivity with flow-BOLD coupling and regional vasculature. Brain Connect. 5, 137–146. https://doi.org/10.1089/brain.2014.0299.

Tambini, A., Nee, D.E., D'Esposito, M., 2017. Hippocampal-targeted theta-burst stimulation enhances associative memory formation. J. Cogn. Neurosci. 30, 1452–1472. https://doi.org/10.1162/jocn_a_01300.

Taylor, K.I., Moss, H.E., Stamatakis, E.A., Tyler, L.K., 2006. Binding crossmodal object features in perirhinal cortex. Proc. Natl. Acad. Sci. 103, 8239–8244. https://doi.org/10.1073/pnas.0509704103.

Tobia, M.J., Yang, Q.X., Karunanayaka, P., 2016. Intrinsic intranasal chemosensory brain networks shown by resting-state functional MRI. Neuroreport 27, 527–531. https://doi.org/10.1097/WNR.0000000000000579.

Tort, A.B.L., Brankačk, J., Draguhn, A., 2018. Respiration-entrained brain rhythms are global but often overlooked. Trends Neurosci. 41, 186–197. https://doi.org/10.1016/j.tins.2018.01.007.

Tristan, C., François, D., Philippe, L., Samuel, G., Corine, A., Nathalie, B., 2009. Respiration-gated formation of gamma and beta neural assemblies in the mammalian olfactory bulb. Eur. J. Neurosci. 29, 921–930. https://doi.org/10.1111/j.1460-9568.2009.06651.x.

Tsanov, M., Chah, E., Reilly, R., O'Mara, S.M., 2014. Respiratory cycle entrainment of septal neurons mediates the fast coupling of sniffing rate and hippocampal theta rhythm. Eur. J. Neurosci. 39, 957–974. https://doi.org/10.1111/ejn.12449.

Uyematsu, S., 1921. A study of the cortical olfactory center: based on two cases of unilateral involement of the olfactory lobe. Arch. Neurol. Psychiatry 6, 146–156. https://doi.org/10.1001/archneurpsyc.1921.02190020029002.

van den Heuvel, M.P., Hulshoff Pol, H.E., 2010. Exploring the brain network: a review on resting-state fMRI functional connectivity. Eur. Neuropsychopharmacol. 20, 519–534. https://doi.org/10.1016/j.euroneuro.2010.03.008.

Vanderwolf, C.H., 1992. Hippocampal activity, olfaction, and sniffing: an olfactory input to the dentate gyrus. Brain Res. 593, 197–208. https://doi.org/10.1016/0006-8993(92)91308-2.

Vanderwolf, C., 2001. The hippocampus as an olfacto-motor mechanism: were the classical anatomists right after all? Behav. Brain Res. 127, 25–47. https://doi.org/10.1016/S0166-4328(01)00354-0.

Varga, S., Heck, D.H., 2017. Rhythms of the body, rhythms of the brain: respiration, neural oscillations, and embodied cognition. Conscious. Cogn. 56, 77–90. https://doi.org/10.1016/j.concog.2017.09.008.

Vaughan, D.N., Jackson, G.D., 2014. The piriform cortex and human focal epilepsy. Front. Neurol. 5, 259. https://doi.org/10.3389/fneur.2014.00259.

Vermetten, E., Bremner, J.D., 2003. Olfaction as a traumatic reminder in posttraumatic stress disorder: case reports and review. J. Clin. Psychiatry 64, 202–207. https://doi.org/10.4088/JCP.v64n0214.

Veyrac, A., Allerborn, M., Gros, A., Michon, F., Raguet, L., Kenney, J., Godinot, F., Thevenet, M., Garcia, S., Messaoudi, B., Laroche, S., Ravel, N., 2015. Memory of occasional events in rats: individual episodic memory profiles, flexibility, and neural substrate. J. Neurosci. 35, 7575–7586. https://doi.org/10.1523/JNEUROSCI.3941-14.2015.

Viczko, J., Sharma, A.V., Pagliardini, S., Wolansky, T., Dickson, C.T., 2014. Lack of respiratory coupling with neocortical and hippocampal slow oscillations. J. Neurosci. 34, 3937–3946. https://doi.org/10.1523/JNEUROSCI.3581-13.2014.

Vinck, M., Oostenveld, R., van Wingerden, M., Battaglia, F., Pennartz, C.M.A., 2011. An improved index of phase-synchronization for electrophysiological data in the presence of volume-conduction, noise and sample-size bias. Neuroimage 55, 1548–1565. https://doi.org/10.1016/j.neuroimage.2011.01.055.

Wang, Q., Sporns, O., Burkhalter, A., 2012. Network analysis of corticocortical connections reveals ventral and dorsal processing streams in mouse visual cortex. J. Neurosci. 32, 4386–4399. https://doi.org/10.1523/JNEUROSCI.6063-11.2012.

Weiss, F., Zamoscik, V., Schmidt, S.N.L., Halli, P., Kirsch, P., Gerchen, M.F., 2020. Just a very expensive breathing training? Risk of respiratory artefacts in functional connectivity-based real-time fMRI neurofeedback. Neuroimage 210, 116580. https://doi.org/10.1016/j.neuroimage.2020.116580.

Wesson, D.W., 2020. The tubular striatum. J. Neurosci. 40, 7379–7386. https://doi.org/10.1523/JNEUROSCI.1109-20.2020.

White, T.L., 1998. Olfactory memory: the long and short of it. Chem. Senses 23, 433–441. https://doi.org/10.1093/chemse/23.4.433.

Willander, J., Larsson, M., 2006. Smell your way back to childhood: autobiographical odor memory. Psychon. Bull. Rev. 13, 240–244. https://doi.org/10.3758/BF03193837.

Wilson, D.A., Sullivan, R.M., 2003. Sensory physiology of central olfactory pathways. In: Doty, R.L. (Ed.), Handbook of Olfaction and Gestation. Marcel Dekker, Inc, New York, pp. 181–201.

Wilson, D.A., Willner, J., Kurz, E.M., Nadel, L., 1986. Early handling increases hippocampal long-term potentiation in young rats. Behav. Brain Res. 21, 223–227. https://doi.org/10.1016/0166-4328(86)90240-8.

Woolrich, M.W., Jbabdi, S., Patenaude, B., Chappell, M., Makni, S., Behrens, T., Beckmann, C., Jenkinson, M., Smith, S.M., 2009. Bayesian analysis of neuroimaging data in FSL. Neuroimage 45, S173–S186. https://doi.org/10.1016/j.neuroimage.2008.10.055.

Yanovsky, Y., Ciatipis, M., Draguhn, A., Tort, A.B.L., Brankačk, J., 2014. Slow oscillations in the mouse hippocampus entrained by nasal respiration. J. Neurosci. 34, 5949–5964. https://doi.org/10.1523/JNEUROSCI.5287-13.2014.

Yeshurun, Y., Lapid, H., Dudai, Y., Sobel, N., 2009. The privileged brain representation of first olfactory associations. Curr. Biol. 19, 1869–1874. https://doi.org/10.1016/j.cub.2009.09.066.

Zelano, C., Bensafi, M., Porter, J., Mainland, J., Johnson, B., Bremner, E., Telles, C., Khan, R., Sobel, N., 2005. Attentional modulation in human primary olfactory cortex. Nat. Neurosci. 8, 114–120. https://doi.org/10.1038/nn1368.

Zelano, C., Jiang, H., Zhou, G., Arora, N., Schuele, S., Rosenow, J., Gottfried, J.A., 2016. Nasal respiration entrains human limbic oscillations and modulates cognitive function. J. Neurosci. 36, 12448–12467. https://doi.org/10.1523/JNEUROSCI.2586-16.2016.

Zhang, Y., Brady, M., Smith, S., 2001. Segmentation of brain MR images through a hidden Markov random field model and the expectation-maximization algorithm. IEEE Trans. Biomed. Eng. 20, 45–57. https://doi.org/10.1109/42.906424.

Zhou, G., Lane, G., Cooper, S.L., Kahnt, T., Zelano, C., 2019a. Characterizing functional pathways of the human olfactory system. Elife 8, e47177. https://doi.org/10.7554/eLife.47177.

Zhou, G., Lane, G., Noto, T., Arabkheradmand, G., Gottfried, J.A., Schuele, S.U., Rosenow, J.M., Olofsson, J.K., Wilson, D.A., Zelano, C., 2019b. Human olfactory-auditory integration requires phase synchrony between sensory cortices. Nat. Commun. 10, 1168. https://doi.org/10.1038/s41467-019-09091-3.

Zucco, G.M., 2003. Anomalies in cognition: olfactory memory. Eur. Psychol. 8, 77–86. https://doi.org/10.1027//1016-9040.8.2.77.